

# A Constructive and Unifying Framework for Zero-Bit Watermarking

Teddy Furon

**Abstract**—In the watermark detection scenario, also known as zero-bit watermarking, a watermark, carrying no hidden message, is inserted in a piece of content. The watermark detector checks for the presence of this particular weak signal in received contents. The article looks at this problem from a classical detection theory point of view, but with side information enabled at the embedding side. This means that the watermark signal is a function of the host content. Our study is twofold. The first step is to design the best embedding function for a given detection function, and the best detection function for a given embedding function. This yields two conditions, which are mixed into one 'fundamental' partial differential equation. It appears that many famous watermarking schemes are indeed solution to this 'fundamental' equation. This study thus gives birth to a constructive framework unifying solutions, so far perceived as very different.

**Index Terms**—Detection theory, Pitman–Noether theorem, zero-bit watermarking.

## I. INTRODUCTION

IN the past six years, side-informed embedding strategies have been shown to greatly improve watermark decoding. They exploit knowledge of the host signal during the construction of the watermark signal. The theory underlying these side-informed schemes was presented in the famous paper “Writing on dirty paper” by M. Costa in 1983. Our work gives some theoretical aspect of the achievable performances when using side information at the embedding side, as in Costa’s correspondence, but for the watermark detection problem (a.k.a. zero-bit watermarking [1, Sec. 2.2.3]). This surprisingly received almost no study compared to the issue of watermark decoding, although it is perceived as a nontrivial problem [2], [3]. Some other exceptions are works from M. Miller *et al.* (embedding cone) [4], JANIS [5], and watermark detection with distortion-compensated dither modulation (DC–DM) schemes [6].

### A. Motivations From the Application Side

The tradeoff between the payload of the hidden message and robustness is a well-known fact in watermarking. The main rationale for zero-bit watermarking is that maximum robustness that a watermarking primitive can inherently offer, is expected as the payload is reduced to the minimum. Here are two application scenarios where zero-bit watermarking might be sufficient

Manuscript received June 6, 2006; revised February 24, 2007. This work was supported by the French national Programme “Sécurité ET Informatique” under Project NEBBIANO, ANR-06-SETIN-009. The associate editor coordinating the review of this manuscript and approving it for publication was Dr. Upamanyu Madhow.

The author is with the TEMICS Project at INRIA, IRISA/TEMICS, Rennes Cedex 35042 (e-mail: teddy.furon@irisa.fr).

Digital Object Identifier 10.1109/TIFS.2007.897272

(i.e., it is not necessary to hide a message, but just the presence of a mark).

Some copy protection platforms [7] use watermarks as flags whose presence warns compliant devices that the piece of content they are dealing with is copyrighted material. Content access and copy protection are tackled by cryptographic primitives. Watermarking just prevents the “analog hole” [8]–[10]. In other words, compliant devices expect three kinds of content: commercial contents which are encrypted and watermarked, free contents which are in the clear and not watermarked, and pirated contents through the “analog hole” which are in the clear but watermarked. Although most digital right management (DRM) systems hide a message such as copy status, we have seen here that the presence of a mark is indeed sufficient.

Copyright protection is the most famous application of watermarking. However, hiding the name of the author in his work is just a fact that has no legal value. In Europe, the author first must be a member of an author society, then he or she registers his or her work. The only legal proof is to give evidence that the suspicious image is indeed a version of a work duly registered in an author society’s database. Consequently, this is a yes or no question, which can be solved by detecting the presence or absence of a watermark previously embedded by an author society.

In these two applications, the presence of a watermark is not a secret, contrary to a steganographic scenario. The attacker obviously knows which content is watermarked. In the copy protection application, for instance, there is no point in attacking a personal video which is of free content, not protected neither by encryption nor by watermarking.

### B. Motivations From the Scientific Side

Zero-bit watermarking is closely related to the detection of weak signals in the noisy environment: the watermark signal is embedded in a host signal, unknown to the detector. Its power is very weak compared to the one of the host. Watermarkers resorted to classical elements of detection theory very early. This includes the use of Neyman–Pearson and Pitman–Noether theorems, calculus of asymptotic efficacy, locally most powerful (LMP) tests [11], and robust statistics [12].

The priority was, at this time, to design a better detector than the classical correlation, which is only optimal for white host signals. To name a few, this includes the works of teams such as Cheng and Huang [13], Briassouli and Strinzis [14], and Barni *et al.* [15]. They assume that the host signals are drawn from a known probability density function (pdf), and they apply the above-mentioned classical elements of detection theory. Huang and Zhang relax this implicit assumption considering that the “real” pdf of the host belongs to a given family of distributions

[16]. Their test is designed to fairly perform for the entire family. This allows encompassing attacks modifying the pdf within the family.

Another track is to see the host signal as a side information only available at embedding. Side information brings huge improvements in watermark decoding. However, its use for zero-bit watermarking has received less interest. Pioneer works are mostly heuristic approaches [4], [17]. More recent works use the binning principle to achieve zero-bit watermarking [6], [18], although J. Eggers notices that the scalar Costa scheme (SCS) is less efficient for zero-bit than for the positive rate watermarking scheme [19, Sec. 3.6]. Indeed, Erez *et al.* prove the optimality of DC-DM based on lattices (those whose Voronoi region asymptotically tends to a hypersphere) for strictly positive rate data hiding as far as an additive white noise attack is considered [20]. In the case of zero-rate watermarking, P. Moulin *et al.* reasonably conjecture that sparse lattice DC-DM is optimal [21]. For zero-bit watermarking, lattice DC-DM achieves high performances showing some host interference rejection [6]. However, there is a loss of efficacy compared to the private setup where side information is also available at the detector.

At first glance, it would seem that the problem of watermark detection is simpler than the decoding of hidden symbols, because the decoder's output belongs to a message space which is bigger than the detector's range  $\mathbb{B} = \{0, 1\}$ . In other words, whereas watermark detection implies a simple binary hypotheses test, the decoding of watermark is a complex multiple hypotheses test.

Yet, almost no theoretical limit (i.e., an equivalent of Costa's result) but for watermark detection, has been shown, except [22, Sec. 2] which only tackles the Gaussian case. N. Merhav mentioned during the WaCha'05 workshop in Barcelona, that zero-bit watermarking is a hard problem whose optimal solution is not known for the moment [2]. Especially, up to now, there is no reason why the binning principle should be optimal, even if, as far as the author knows from the literature, it has the best performances against an additive white Gaussian noise (AWGN) attack. Yet, DC-DM schemes are known to be weak against scale gain attack.

## II. STRATEGY AND NOTATION

Our goal is not to derive an accurate statistical model of the host signal as performed in the previously mentioned prior works. To the contrary, very basic assumptions (Gaussian distribution or flat-host assumption) are in order, allowing us to stress the major role of side information at the embedding side. While the binning scheme is commonly used to exploit side information, it is not the only way. Our approach is indeed closer to the theory of weak signal detection.

### A. Embedding Side

The embedder transforms an original host signal  $\mathbf{s}$  into watermarked content  $\mathbf{y} = \mathbf{f}(\mathbf{s}) = \mathbf{s} + \mathbf{x}$ . The host signal or channel state  $\mathbf{s}$  is a vector of  $n$  components of the original content, modeled as random variables. The notational key of the article is to

decompose the watermark signal  $\mathbf{x}$  as a unit power vector  $\mathbf{w}$  and amplitude  $\theta$

$$\mathbf{f}(\mathbf{s}) = \mathbf{s} + \mathbf{x} = \mathbf{s} + \theta\mathbf{w}(\mathbf{s}). \quad (1)$$

where  $\mathbf{w}$  is a smooth function from  $\mathbb{R}^n$  to  $\mathbb{R}^n$ , with the constraints  $\mathbb{E}_{\mathbf{S}}\{\mathbf{w}(\mathbf{s})\} = 0$  and  $\mathbb{E}_{\mathbf{S}}\{\|\mathbf{w}(\mathbf{s})\|^2\} = n$ . This vector gives a direction pointing to an acceptance region of  $\mathbb{R}^n$ , toward which the host signal should be pushed. The scalar  $\theta$  controls the gain or amplitude of the watermark signal. Theoretical frameworks often use a constant  $\theta = \sqrt{P}$ , where  $P$  is the fixed power of  $\mathbf{x}$ . Yet, in practice, host contents might support different watermark power depending on their individual masking property. This change might even occur within a content, such that we should resort to a vector  $\boldsymbol{\theta} = (\theta_1, \dots, \theta_n)$  gathering positive and small gains affecting each sample. We restrict our study to scalar gain for the sake of simplicity, but the results of this paper can be easily extended to a vector gain. In this case, one might consider  $\theta$  as the average gain.

Both parts of the watermark signal depend on the host content, either through side information, or for some perceptual reasons. Unfortunately, in blind schemes, side information is not made available at the detection side. Moreover, we wish to maintain a low detector's complexity, which prevents the use of a human visual or auditive system in order to recreate an estimate of  $\theta$  based on the received content. The only fact the detector knows is that the watermark amplitude  $\theta$  is positive and small. We believe this model allows great flexibility which eases practical implementations of watermarking schemes.

### B. Detection Side

Upon the receipt of signal  $\mathbf{r}$ , the detector makes a binary decision  $d = 1$  ( $d = 0$ ) meaning that, according to the detector, the piece of content under scrutiny is watermarked (respectively, it has not been watermarked). There are two hypotheses: Under hypothesis  $\mathcal{H}_0$ , the detector receives an original content  $\mathbf{r} = \mathbf{r}_0 = \mathbf{s}$  (see the end of Section I-A for justifications), whereas under hypothesis  $\mathcal{H}_1$ , the detector receives watermarked and possibly attacked content  $\mathbf{r} = \mathbf{r}_1$ . The probability of false alarm  $P_{fa}$  and power of the test  $P_p$  are given by

$$P_{fa} = \Pr\{d = 1|\mathcal{H}_0\}; \quad P_p = \Pr\{d = 1|\mathcal{H}_1\}. \quad (2)$$

Once again, in zero-bit watermarking, no symbol is transmitted. Our problem is then fundamentally different from the communication of one bit because, under hypothesis  $\mathcal{H}_0$ , no processing is applied and  $\mathbf{s}$ , given by nature, is directly sent to the detector.

We assume that the detector has the structure of a Neyman-Pearson test. First, it applies a detection function  $t$  mapping from  $\mathbb{R}^n$  to  $\mathbb{R}$ . Then, this scalar is compared to a threshold  $\tau$ :  $d = 1$  if  $t(\mathbf{r}) > \tau$ ,  $d = 0$  else. The threshold is given by the constraint of a significance level  $\alpha$  such that  $P_{fa} = \mathbb{E}_D\{d|\mathcal{H}_0\} \leq \alpha$ . Note that for a given detection function, this threshold does not depend on what happens under hypothesis  $\mathcal{H}_1$  (embedding function  $\mathbf{w}$ , watermark's amplitude  $\theta$ ). Moreover, we assume

without loss of generality, that, under hypothesis  $\mathcal{H}_0$ ,  $t(\mathbf{r})$  is a centered random variable with unit variance

$$\mathbb{E}_{\mathbf{R}}\{t(\mathbf{r})|\mathcal{H}_0\} = 0, \quad \text{Var}\{t(\mathbf{r})|\mathcal{H}_0\} = 1. \quad (3)$$

If not the case, it is easy to build the test  $\tilde{t}(\mathbf{r}) = (t(\mathbf{r}) - \mathbb{E}_{\mathbf{R}}\{t(\mathbf{r})|\mathcal{H}_0\})/\sqrt{\text{Var}\{t(\mathbf{r})|\mathcal{H}_0\}}$ .

### C. Pitman–Noether Efficacy

In this article, the tests are compared asymptotically for  $n \rightarrow +\infty$ . The Pitman–Noether theorem indicates that the best test has the higher efficacy  $\eta$ , whose general definition is given by [11, Sect. III-C3]: See equation (4) at the bottom of the page, where  $m$  is the first integer for which the  $m$ th derivative of  $\mathbb{E}_{\mathbf{R}}\{t(\mathbf{r})|\mathcal{H}_1\}$  is not null, and  $\delta$  a positive scalar such that the limit is not null. In our problem, it is not unreasonable to assume  $m = 1$  and  $\delta = 1/2$  because the expectation of the detection function grows with  $\sqrt{n}$  as  $\text{Var}\{t(\mathbf{r})|\mathcal{H}_0\}$  has been set to one for all  $n$ . This is at least true for well-known watermarking schemes. We are not able to find a counter-example (i.e., a watermarking scheme having a better growth rate than  $\sqrt{n}$ ). Therefore, we restrict our analysis to  $\delta = 1/2$ .

The Pitman–Noether theorem holds for a composite one-sided hypothesis test. In Section II-A, motivations clearly show that our problem is not a simple hypothesis test ( $\mathcal{H}_0 : \theta = 0$  versus  $\mathcal{H}_1 : \theta = \sqrt{P}$  fixed), but a composite one-sided hypothesis test ( $\mathcal{H}_0 : \theta = 0$  versus  $\mathcal{H}_1 : \theta > 0$ ).

Last but not least, the proof of this theorem is based on an asymptotic study where the alternative hypothesis  $\mathcal{H}_1$  has a vanishing parameter  $\theta_n = kn^{-\delta}$ , with  $k$  a positive constant. Important assumptions are the following regularity conditions:

$$\lim_{n \rightarrow \infty} \left( \frac{\frac{\partial}{\partial \theta} \mathbb{E}_{\mathbf{R}}\{t(\mathbf{r})|\mathcal{H}_1\} \Big|_{\theta=\theta_n}}{\frac{\partial}{\partial \theta} \mathbb{E}_{\mathbf{R}}\{t(\mathbf{r})|\mathcal{H}_1\} \Big|_{\theta=0}} \right) = 1 \quad (5)$$

$$\lim_{n \rightarrow \infty} \left( \frac{\text{Var}\{t(\mathbf{r})|\mathcal{H}_1\}}{\text{Var}\{t(\mathbf{r})|\mathcal{H}_0\}} \right) = 1 \quad (6)$$

and that  $t(\mathbf{r}) - \mathbb{E}_{\mathbf{R}}\{t(\mathbf{r})\}$  tends (convergence in law), as  $n \rightarrow \infty$ , to a normal variable, both under  $\mathcal{H}_1$  and under  $\mathcal{H}_0$ .

We also define the efficiency per element (a.k.a. the differential detector signal-to-noise ratio) in the same way as the efficacy but without the limit, such that in our case

$$\eta = \frac{1}{n} \left[ \frac{\partial}{\partial \theta} \mathbb{E}_{\mathbf{R}}\{t(\mathbf{r})|\mathcal{H}_1\} \Big|_{\theta=0} \right]^2. \quad (7)$$

### III. DETECTION OF THE WEAK SIGNAL DEPENDENT ON SIDE INFORMATION

The goal of this section is to give the expressions for the best detection and the best embedding functions. We mean “best”

in the sense of the Pitman–Noether theorem (i.e., such as they maximized the efficiency per element).

This section does not consider any attack. Hence, the Pitman–Noether theorem considers signals  $r_0 = \mathbf{s}$  and  $\mathbf{r}_1 = \mathbf{y} = \mathbf{s} + \theta_n \mathbf{w}(\mathbf{s})$ , with  $\mathbb{E}_{\mathbf{S}}\{\|\mathbf{w}(\mathbf{s})\|^2\} = n$  and  $\theta_n = k/\sqrt{n}$ ,  $k > 0$ . It means that the proof of this theorem fixes the embedding distortion to  $D_E = \theta_n^2 n = k^2$ , but as  $n$  increases, the power of the watermarking signal vanishes.

#### A. Best Detector for a Given Embedding Function

In this subsection, embedding function  $\mathbf{w}$  is fixed. A well-known corollary of the Pitman–Noether theorem [11, Sec. III-C3] states that the LMP test in  $\theta = 0$  is asymptotically the best. A Cauchy–Schwarz inequality gives

$$\begin{aligned} & \frac{\partial}{\partial \theta} \mathbb{E}_{\mathbf{R}}\{t(\mathbf{r})|\mathcal{H}_1\} \Big|_{\theta=0} \\ &= \int_{\mathbb{R}^n} t(\mathbf{r}) \frac{\partial}{\partial \theta} p(\mathbf{r}|\mathcal{H}_1) \Big|_{\theta=0} d\mathbf{r} \end{aligned} \quad (8)$$

$$\begin{aligned} & \leq \sqrt{\int_{\mathbb{R}^n} t(\mathbf{r})^2 p(\mathbf{r}|\mathcal{H}_0) d\mathbf{r}} \\ & \times \sqrt{\int_{\mathbb{R}^n} p(\mathbf{r}|\mathcal{H}_0) \left( \frac{1}{p(\mathbf{r}|\mathcal{H}_0)} \frac{\partial}{\partial \theta} p(\mathbf{r}|\mathcal{H}_1) \Big|_{\theta=0} \right)^2 d\mathbf{r}} \end{aligned} \quad (9)$$

$$= \sqrt{\int_{\mathbb{R}^n} p(\mathbf{r}|\mathcal{H}_0) \left( \frac{1}{p(\mathbf{r}|\mathcal{H}_0)} \frac{\partial}{\partial \theta} p(\mathbf{r}|\mathcal{H}_1) \Big|_{\theta=0} \right)^2 d\mathbf{r}} \quad (10)$$

with equality for the LMP test

$$t(\mathbf{r}) = k_t \frac{1}{p(\mathbf{r}|\mathcal{H}_0)} \frac{\partial p(\mathbf{r}|\mathcal{H}_1)}{\partial \theta} \Big|_{\theta=0} \quad (11)$$

where  $k_t$  is a positive constant whose role is explained below. The use of the LMP with  $\theta = 0$  is reinforced in practice by the fact that the watermark power is very weak compared to the host power.

When there is no attack,  $p(\mathbf{r}|\mathcal{H}_0) = p_{\mathbf{S}}(\mathbf{r})$  and  $p(\mathbf{r}|\mathcal{H}_1) = p_{\mathbf{Y}}(\mathbf{r})$ . We assume there exists  $\bar{\theta} > 0$ , such that function  $\mathbf{f}(\mathbf{s})$  is invertible at least when  $0 \leq \theta \leq \bar{\theta}$ :  $\mathbf{s} = \mathbf{f}^{-1}(\mathbf{y})$ . This allows writing  $p_{\mathbf{Y}}(\mathbf{r}) = p_{\mathbf{S}}(\mathbf{f}^{-1}(\mathbf{r})) |J_{\mathbf{f}^{-1}}(\mathbf{r})|$ , with the last term being the determinant of the Jacobian matrix of  $\mathbf{f}^{-1}$  taken at  $(\mathbf{r}, \theta)$ . Developing this last equation (see Appendix A), we finally obtain these expressions

$$t(\mathbf{r}) = -k_t \frac{\nabla p_{\mathbf{S}}(\mathbf{r})^T}{p_{\mathbf{S}}(\mathbf{r})} \mathbf{w}(\mathbf{r}) - k_t \text{div}(\mathbf{w}(\mathbf{r})) \quad (12)$$

$$= -k_t \frac{\text{div}(p_{\mathbf{S}}(\mathbf{r}) \mathbf{w}(\mathbf{r}))}{p_{\mathbf{S}}(\mathbf{r})}. \quad (13)$$

The first term of (12) corresponds to the classical nonlinear correlation-based LMP test [13]–[15], whereas the second term is

$$\bar{\eta} = \left( \lim_{n \rightarrow \infty} n^{-m\delta} \frac{\partial^m}{\partial \theta^m} \mathbb{E}_{\mathbf{R}}\{t(\mathbf{r})|\mathcal{H}_1\} \Big|_{\theta=0} \text{Var}\{t(\mathbf{r})|\mathcal{H}_0\}^{-1/2} \right)^{1/m\delta} \quad (4)$$

not null whenever side information is enabled at the embedding side.

Let  $\mathcal{B}_n(R)$  be the ball of radius  $R$  centered on  $\mathbf{0}$ ,  $\mathcal{S}_n(R)$  the associated hypersphere, and  $E(R) = \int_{\mathcal{B}_n(R)} t(\mathbf{r}) p_{\mathcal{S}}(\mathbf{r}) d\mathbf{r}$ . Then, thanks to the Gauss theorem, we have

$$|E(R)| = k_t \left| \int_{\mathcal{B}_n(R)} \operatorname{div}(p_{\mathcal{S}}(\mathbf{r}) \mathbf{w}(\mathbf{r})) d\mathbf{r} \right| \quad (14)$$

$$= k_t \left| \int_{\mathcal{S}_n(R)} p_{\mathcal{S}}(\mathbf{r}) \mathbf{w}(\mathbf{r})^T \mathbf{e}(\mathbf{r}) d\mathbf{r} \right| \quad (15)$$

$$\leq k_t \int_{\mathcal{S}_n(R)} p_{\mathcal{S}}(\mathbf{r}) \|\mathbf{w}(\mathbf{r})\| d\mathbf{r} \quad (16)$$

with  $\mathbf{e}(\mathbf{r})$  being the unit normal vector at position  $\mathbf{r}$  on  $\mathcal{S}_n(R)$ .  $E\{\|\mathbf{w}(\mathbf{r})\|^2\} < \infty$  implies that  $\lim_{R \rightarrow +\infty} E(R) = 0$ . This shows that the expectation of the detection function given by (13) is zero under hypothesis  $\mathcal{H}_0$ , as required in Section II-B. The constant  $k_t$  enforces that  $\operatorname{Var}\{t(\mathbf{r})|\mathcal{H}_0\} = 1$

$$k_t = \left( \int_{\mathbb{R}^n} \frac{1}{p(\mathbf{r}|\mathcal{H}_0)} \left[ \frac{\partial p(\mathbf{r}|\mathcal{H}_1)}{\partial \theta} \right]_{\theta=0}^2 d\mathbf{r} \right)^{-1/2}. \quad (17)$$

Finally, (7), (11), and (17) give the efficiency per element for such tests

$$\eta = n^{-1} k_t^{-2}. \quad (18)$$

### B. Best Embedding Function for a Given Detection Function

The detection function  $t$  being given (such that  $t(\mathbf{r}_0)$  is a centered random variable with unit variance), we write

$$\begin{aligned} \left. \frac{\partial}{\partial \theta} \mathbb{E}_{\mathbf{R}}\{t(\mathbf{r})|\mathcal{H}_1\} \right|_{\theta=0} &= \mathbb{E}_{\mathcal{S}} \left\{ \left. \frac{\partial}{\partial \theta} t(\mathbf{s} + \theta \mathbf{w}(\mathbf{s})) \right|_{\theta=0} \right\} \\ &= \mathbb{E}_{\mathcal{S}} \{ \mathbf{w}(\mathbf{s})^T \nabla t(\mathbf{s}) \}. \end{aligned} \quad (19)$$

It appears that, for a given  $t$ , it is important to let  $\mathbf{w}(\mathbf{s}) \propto \nabla t(\mathbf{s})$ ,  $\forall \mathbf{s} \in \mathbb{R}^n$ . The efficiency per element is then upperbounded by the following Cauchy–Schwarz inequality:

$$\begin{aligned} \eta &= \frac{1}{n} \left( \int_{\mathbb{R}^n} p_{\mathcal{S}}(\mathbf{s}) \|\mathbf{w}(\mathbf{s})\| \|\nabla t(\mathbf{s})\| d\mathbf{s} \right)^2 \\ &\leq \int_{\mathbb{R}^n} p_{\mathcal{S}}(\mathbf{s}) \|\nabla t(\mathbf{s})\|^2 d\mathbf{s} \end{aligned} \quad (20)$$

with equality when

$$\mathbf{w}(\mathbf{s}) = k_w \nabla t(\mathbf{s}), \quad \forall \mathbf{s} \in \mathbb{R}^n \quad (21)$$

where  $k_w$  is a normalizing constant to achieve  $\mathbb{E}_{\mathcal{S}}\{\|\mathbf{w}(\mathbf{s})\|^2\} = n$ :

$$k_w = \sqrt{\frac{n}{\mathbb{E}_{\mathcal{S}}\{\|\nabla t(\mathbf{s})\|^2\}}}. \quad (22)$$

Equations (20) and (22) give the efficiency per element for such tests

$$\eta = n k_w^{-2} = \mathbb{E}_{\mathcal{S}}\{\|\nabla t(\mathbf{s})\|^2\}. \quad (23)$$

### C. Synthesis

For the moment, we know how to design the best embedding function for a given detection function, and how to design the best detection function for a given embedding function. This is reminiscent of the Lloyd–Max algorithm in quantization. However, dealing with closed-form equations, we can insert (21) in (13), yielding a partial differential equation, that we loosely name “fundamental equation of zero-bit watermarking”

$$p_{\mathcal{S}}(\mathbf{r}) t(\mathbf{r}) + k_t k_w \operatorname{div}(p_{\mathcal{S}}(\mathbf{r}) \nabla t(\mathbf{r})) = 0, \quad \forall \mathbf{r} \in \mathbb{R}^n. \quad (24)$$

Hence, the best couple of detection/embedding functions  $\{t, \mathbf{w}\}$  is  $\{t^*, k_w \nabla t^*\}$ , with  $t^*$  a fundamental solution (i.e., a solution of (24)). Note that (18) and (23) are still valid. Therefore, it is possible to build a scheme of a given  $\eta$  (virtually, as high as possible), provided (24) admits a solution with  $k_w k_t = \eta^{-1}$ . The fundamental equation can also be written as

$$\eta t(\mathbf{r}) + \frac{\nabla p_{\mathcal{S}}(\mathbf{r})^T}{p_{\mathcal{S}}(\mathbf{r})} \nabla t(\mathbf{r}) + \nabla^2 t(\mathbf{r}) = 0 \quad (25)$$

with  $\nabla^2 t(\mathbf{r})$  being the Laplacian of  $t(\mathbf{r})$ .

### D. Geometric Property of Fundamental Solutions

A nice property induced by the fundamental equation is that a pair of its solutions with different efficiencies per element are orthonormal for the scalar product  $\langle \cdot, \cdot \rangle$  defined here for two functions  $g$  and  $h$  by

$$\langle g, h \rangle = \mathbb{E}_{\mathbf{R}}\{g(\mathbf{r})h(\mathbf{r})|\mathcal{H}_0\}. \quad (26)$$

Denote  $L[t] = \operatorname{div}(p_{\mathcal{S}}(\mathbf{r}) \nabla t(\mathbf{r}))$ . This differential operator is symmetric if  $\int_{\mathbb{R}^n} t_i(\mathbf{r}) L[t_j](\mathbf{r}) d\mathbf{r} = \int_{\mathbb{R}^n} L[t_i](\mathbf{r}) t_j(\mathbf{r}) d\mathbf{r}$ . In our case

$$\begin{aligned} \int_{\mathbb{R}^n} t_i(\mathbf{r}) L[t_j](\mathbf{r}) d\mathbf{r} - \int_{\mathbb{R}^n} t_j(\mathbf{r}) L[t_i](\mathbf{r}) d\mathbf{r} \\ = \int_{\mathbb{R}^n} \operatorname{div}(p_{\mathcal{S}}(\mathbf{r}) (t_i(\mathbf{r}) \nabla t_j(\mathbf{r}) - t_j(\mathbf{r}) \nabla t_i(\mathbf{r}))) d\mathbf{r}. \end{aligned} \quad (27)$$

The symmetry is enabled for functions  $t_i, t_j$  if the last term, denoted by  $C$ , is zero. Let us write it as a limit

$$\begin{aligned} C &= \int_{\mathbb{R}^n} \operatorname{div}(p_{\mathcal{S}}(\mathbf{r}) (t_i(\mathbf{r}) \nabla t_j(\mathbf{r}) - t_j(\mathbf{r}) \nabla t_i(\mathbf{r}))) d\mathbf{r} \\ &= \lim_{R \rightarrow \infty} \int_{\mathcal{B}_n(R)} \operatorname{div}(p_{\mathcal{S}}(\mathbf{r}) (t_i(\mathbf{r}) \nabla t_j(\mathbf{r}) - t_j(\mathbf{r}) \nabla t_i(\mathbf{r}))) d\mathbf{r} \\ &= \lim_{R \rightarrow \infty} \int_{\mathcal{S}_n(R)} p_{\mathcal{S}}(\mathbf{r}) (t_i(\mathbf{r}) \nabla t_j(\mathbf{r})^T \mathbf{e}(\mathbf{r}) - t_j(\mathbf{r}) \nabla t_i(\mathbf{r})^T \mathbf{e}(\mathbf{r})) d\mathbf{r}. \end{aligned} \quad (28)$$

The Gauss theorem gives the later equation. Assuming that the pdf of the host vanishes more quickly than the norm  $\|t_i(\mathbf{r})\nabla t_j(\mathbf{r})\|$ , we suppose in the sequel that the symmetry property is enabled for the solutions of the fundamental equation. Then, (24) in (27) gives

$$\begin{aligned} & \int_{\mathbb{R}^n} t_i(\mathbf{r})L[t_j](\mathbf{r})d\mathbf{r} - \int_{\mathbb{R}^n} t_j(\mathbf{r})L[t_i](\mathbf{r})d\mathbf{r} \\ &= - \int_{\mathbb{R}^n} t_i(\mathbf{r})\cdot\eta_j p_S(\mathbf{r})t_j(\mathbf{r})d\mathbf{r} + \int_{\mathbb{R}^n} t_j(\mathbf{r})\cdot\eta_i p_S(\mathbf{r})t_i(\mathbf{r})d\mathbf{r} \\ &= (\eta_i - \eta_j)\langle t_i, t_j \rangle = 0. \end{aligned} \quad (29)$$

The restriction to normalized detection functions and this last equation imply that  $\langle t_i, t_j \rangle = \delta(j-i)$ , where  $\delta$  is the Kronecker delta function. Hence, the solutions of the fundamental equation with different efficiencies per element constitute a family of orthonormal functions (Section IV-BI even shows orthonormal functions sharing the same efficiency), if the symmetry property holds for all pairs of elements of this family.

#### IV. SOME SOLUTIONS OF THE FUNDAMENTAL EQUATION OF ZERO-BIT WATERMARKING

We are not able to find a general solution of the fundamental equation. However, in some cases, we show some examples of the solution in this section.

##### A. Scalar Case

To avoid multiplication of notation, we use the same letter to denote the scalar version of the previously mentioned vectorial functions.

We suppose here that the host samples are i.i.d. such that  $p_S(\mathbf{s}) = \prod_{i=1}^n p_S(s_i)$ . Moreover, our strategy is to maintain this statistical independence while embedding the watermark  $\mathbf{w}(\mathbf{s}) = (\epsilon_1 w(s_1), \dots, \epsilon_n w(s_n))^T$ , where  $\epsilon$  is a secret vector with, for instance,  $\epsilon_i = \pm 1 \forall i \in \{1, \dots, n\}$ . Equation (12) shows that the detection function is indeed a sum  $t(\mathbf{r}) = \sum_{i=1}^n \epsilon_i t(r_i)$ ; and (25) boils down to a scalar second-order ordinary differential equation with nonconstant coefficients

$$\eta t(r) + \frac{p'_S(r)}{p_S(r)} t'(r) + t''(r) = 0. \quad (30)$$

1) *Gaussian Case:* Assume that  $s \sim \mathcal{N}(0, \sigma_x^2)$ . Equation (25) becomes even simpler:  $\eta t(r) - r t'(r)/\sigma_x^2 + t''(r) = 0$ . The solution is a linear combination of two “independent” (i.e., their Wronskian is not null) confluent hypergeometric functions of the first kind taken in  $r^2/2$

$$t^{(a)}(r) = k_{t_1} \cdot {}_1F_1\left(-\frac{\sigma_x^2 \eta}{2}, \frac{1}{2}, \frac{r^2}{2\sigma_x^2}\right) \quad (31)$$

$$t^{(b)}(r) = k_{t_2} \cdot r \cdot {}_1F_1\left(\frac{1 - \sigma_x^2 \eta}{2}, \frac{3}{2}, \frac{r^2}{2\sigma_x^2}\right). \quad (32)$$

If  $\sigma_x^2 \eta$  is an even integer,  $t^{(a)}$  is a polynomial function. If  $\sigma_x^2 \eta$  is an odd integer,  $t^{(b)}$  is a polynomial function. Another way to see this is to recognize this later differential equation as the

TABLE I  
POLYNOMIAL SOLUTIONS OF THE SCALAR GAUSSIAN CASE  $s \sim \mathcal{N}(0, 1)$

$\eta$	$w(s)$	$t(r)$	$\text{Var}\{t(r) \mathcal{H}_1\}$
1	1	$r$	1
2	$s$	$\frac{-1+r^2}{\sqrt{2}}$	$(1+\theta)^4$
3	$\frac{-1+s^2}{\sqrt{2}}$	$\frac{-3r+r^3}{\sqrt{6}}$	$1+66\theta^2+O(\theta^4)$
4	$\frac{-3s+s^3}{\sqrt{6}}$	$\frac{3-6r^2+r^4}{2\sqrt{6}}$	$1+12\sqrt{6}\theta+608\theta^2+O(\theta^3)$
5	$\frac{3-6s^2+s^4}{2\sqrt{6}}$	$\frac{15r-10r^3+r^5}{2\sqrt{30}}$	$1+5470\theta^2+O(\theta^4)$
6	$\frac{15s-10s^3+s^5}{2\sqrt{30}}$	$\frac{-15+45r^2-15r^4+r^6}{12\sqrt{5}}$	$1+40\sqrt{30}\theta+49122\theta^2+O(\theta^3)$
7	$\frac{-15+45s^2-15s^4+s^6}{12\sqrt{5}}$	$\frac{-105r+105r^3-21r^5+r^7}{12\sqrt{35}}$	$1+441392\theta^2+O(\theta^4)$

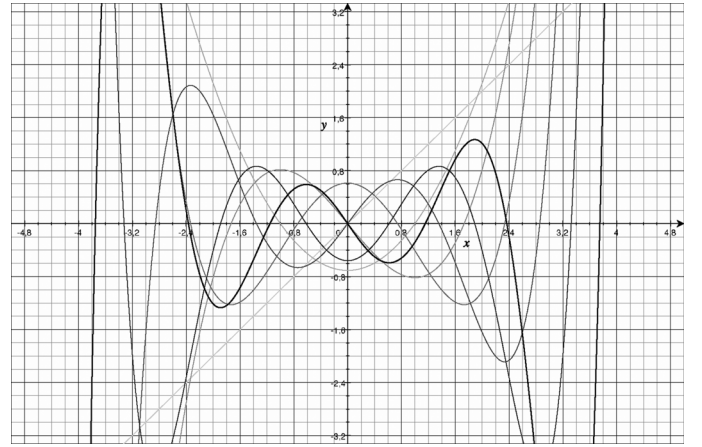


Fig. 1. Plot of the detection function  $r \rightarrow t(r)$  for the seven first elements of the polynomial family as listed in Table I. Darker lines correspond to higher orders.

Hermite equation when  $\eta$  is a positive integer and  $\sigma_x^2 = 1$ . Therefore, if  $\eta\sigma_x^2 = k \in \mathbb{N}$ ,  $t_k(r) = \kappa_k H_k(r/\sigma_x)$ ,  $H_k$  being the Hermite polynomial of order  $k$ . This family of polynomials is known to be orthogonal with a weighting function<sup>1</sup>  $\exp(-r^2/2)$ . In our context, this is confirmed by (28), which reduces to the value of the integrand on the boundaries on an increasing interval of  $\mathbb{R}$ . The condition  $C = 0$  is satisfied because  $\lim_{r \rightarrow \infty} r^m \exp(-r^2/2\sigma_x^2) = 0, \forall m \in \mathbb{N}$ . In the sequel, we call this set of fundamental solutions the “polynomial family.”

Table I gives the expressions of the first elements of this family and their associated embedding function. Fig. 1 shows a plot of the detection function of these first elements.

The first line of this table is the well-known direct SS scheme with a linear correlator, optimal detector in the Gaussian independent and identically distributed (i.i.d.) case. The second line is known as the proportional or multiplicative embedding, first proposed in [23, Sec. 4.2] for perceptual reasons (i.e., it is known that a greater embedding power is not visible when watermarking wavelet coefficients with proportional embedding compared to simple additive embedding). A higher efficiency per element is another inherent advantage of proportional embedding. The remaining lines of this table generalize this idea to new schemes (as far as the author knows).

<sup>1</sup>This is the probabilists’ definition of Hermite polynomials. However, these polynomials take different forms according to the chosen standardization. For instance,  $\kappa_k = 1/\sqrt{k!}$  when the coefficient of highest order of  $H_k$  is set to 1.

2) *Uniform Case*: The classical “flat-host” assumption used in the DC–DM scheme studies states that the host pdf is a piecewise constant function. More precisely, we assume here that the host pdf can be written as  $p_S(s) = \sum_{i=-\infty}^{+\infty} P_i \Pi_i(s)$ , with  $\Pi_i$  being the indicator function of the elementary interval  $[(\pi/\sqrt{\eta})i, (\pi/\sqrt{\eta})(i+1))$ , and  $\sum_{i=-\infty}^{+\infty} P_i = \sqrt{\eta}/\pi$ . In this case, (25) defined almost everywhere,<sup>2</sup> is a lot simpler  $\eta t(r) + t''(r) = 0$ , whose obvious solution<sup>3</sup> is  $t(r) = \sqrt{2} \cos(\sqrt{\eta}r)$  and, hence,  $w(s) = -\sqrt{2} \sin(\sqrt{\eta}s)$ . Although these are not exactly the sawtooth embedding function of the scalar DC–DM (a.k.a. SCS), we find at least periodic functions.

If the “flat-host” assumption holds on the above partition of  $\mathbb{R}$ , then it also holds on the finer partition  $\bigcup_{i=-\infty}^{+\infty} [(\pi/k\sqrt{\eta})i, (\pi/k\sqrt{\eta})(i+1))$ ,  $k \in \mathbb{N}$ . This gives birth to another fundamental solution  $t_k(r) = \sqrt{2} \cos(k\sqrt{\eta}r)$ , whose efficiency per element is  $k^2$  greater. We call the sinusoidal family the set of fundamental solutions  $t_k$  indexed with integers. Once again, elements of this family are orthonormal

$$\begin{aligned} \langle t_k, t_\ell \rangle &= \sum_i 2P_i \int_{i\pi/\sqrt{\eta}}^{(i+1)\pi/\sqrt{\eta}} \cos(k\sqrt{\eta}r) \cos(\ell\sqrt{\eta}r) dr \\ &= \delta(k - \ell). \end{aligned} \quad (33)$$

## B. Vector Case

Section IV-A uses the Cartesian system where the embedding processes in a sample wise manner. We generalize this idea to block-based watermarking schemes assuming there exists an integer  $p$  dividing  $n$  so that  $\mathbb{R}^n = \mathbb{R}^p \times \mathbb{R}^p \cdots \times \mathbb{R}^p$  and that  $p_S(\mathbf{s}) = \prod_{i=1}^{n/p} p(s_{(i-1)p+1}, \dots, s_{(i-1)p+p})$ . If  $t^{(p)}$  is a solution of the fundamental equation in  $\mathbb{R}^p$  with a given efficiency, then  $t^{(n)}(\mathbf{r}) = \sqrt{p/n} \sum_{i=1}^{n/p} t^{(p)}(r_{(i-1)p+1}, \dots, r_{(i-1)p+p})$  is a solution in  $\mathbb{R}^n$  yielding the same efficiency. This realizes a statistically independent embedding in the sense that the block of  $p$  watermark samples only depends on the same block of  $p$  host samples. The issue is now on finding solutions  $t^{(p)}$ . A usual technique is the separation of variables method in a specific orthogonal coordinate system [24].

1) *Separation of Variables*: Classically, the separation of variables method considers a solution  $t^{(p)}(\mathbf{r}) = \prod_{i=1}^p t_{\eta_i}(r_i)$ , where each  $t_{\eta_i}$  has to satisfy (30) with its own efficiency  $\eta_i$ . The resulting efficiency of  $t^{(p)}$  is then  $\eta = \sum_{i=1}^p \eta_i$ . For white Gaussian hosts, this gives birth to an extension of the polynomial family which is indeed based on the multivariate Hermite polynomials, indexed by the  $n/p$ -uple  $\mathbf{k} \in \mathbb{N}^p$ :  $H_{\mathbf{k}}(\mathbf{r}) = \prod_{i=1}^{n/p} H_{k_i}(r_i)$ . Two different elements of this family are orthogonal for the scalar product (26), even if they share the same efficiency per element.

This extension of the polynomial family is illustrated in the following example: If  $\mathbf{S} \sim \mathcal{N}(\mathbf{0}, \sigma_x^2 \mathbf{I}_n)$ , then  $\nabla p_S(\mathbf{r}) = -p_S(\mathbf{r})\mathbf{r}/\sigma_x^2$ , and (24) becomes  $\eta t(\mathbf{r}) - \mathbf{r}^T \nabla t(\mathbf{r})/\sigma_x^2 + \nabla^2 t(\mathbf{r}) = 0$ . JANIS, a zero-bit watermarking

scheme heuristically invented some years ago [5], [17], is a fundamental solution. Its detection function is the following:

$$t(\mathbf{r}) = \sqrt{\frac{p}{n}} \sum_{i=1}^{n/p} \prod_{j=1}^p \frac{r_{(i-1)p+j}}{\sigma_x}. \quad (34)$$

Note that  $r_j$  appears only once in the detection function  $\forall j \in \{1, \dots, n\}$ . It is easy to see that  $\mathbf{r}^T \nabla t(\mathbf{r}) = pt(\mathbf{r})$  and  $\nabla^2 t(\mathbf{r}) = 0$ . Thus, JANIS with order  $p$  is a solution to (24) provided that  $\eta \sigma_x^2 = p$ . This can be interpreted as follows: this is a block-based watermarking scheme built on the  $p$ -multivariate Hermite polynomial  $H_{(1, \dots, 1)}$ . This theoretical framework proves the optimality of the heuristic JANIS scheme.

The separation of variables can be performed on another coordinate system. The following spherical coordinate system  $(\rho, \theta_1, \dots, \theta_{p-1})$  is adapted to isotropic host distributions, that is,  $p_S(\mathbf{s}) = f(\rho)$  with  $\rho = \|\mathbf{s}\|$ :

$$\begin{aligned} r_1 &= \rho \sin \theta_{p-1} \sin \theta_{p-2} \cdots \sin \theta_2 \sin \theta_1 \\ r_2 &= \rho \sin \theta_{p-1} \sin \theta_{p-2} \cdots \sin \theta_1 \cos \theta_1 \\ r_3 &= \rho \sin \theta_{p-1} \sin \theta_{p-2} \cdots \cos \theta_2 \\ &\vdots \\ r_{p-1} &= \rho \sin \theta_{p-1} \cos \theta_{p-2} \\ r_p &= \rho \cos \theta_{p-1}. \end{aligned}$$

For instance, we seek a function  $t(\mathbf{r}) = t(\rho, \theta_{p-1}) = U(\rho)V(\theta_{p-1})$ , which depends on two simple statistics  $\rho = \sum_{i=1}^p r_i^2$  and  $\theta_{p-1} = \arccos(\mathbf{r}^T \mathbf{e}_p / \|\mathbf{r}\|)$ .  $\mathbf{e}_p$  is a secret unit vector shared by the embedder and the detector taken as the  $p$ th element of the canonical basis (i.e., in the Cartesian coordinate system). Separating variables in (25) yields two equations

$$\begin{aligned} KV(\theta) + (p-2) \cot \theta V'(\theta) + V''(\theta) &= 0 \\ (\eta \rho^2 - K)U(\rho) + \left( (p-1)\rho + \rho^2 \frac{f'(\rho)}{f(\rho)} \right) U'(\rho) + \rho^2 U''(\rho) &= 0 \end{aligned} \quad (35)$$

with  $K \in \mathbb{R}$ . The choice  $U(\rho) = k_t \rho^2$  and  $V(\theta) = p \cos^2 \theta - 1$  is a solution provided  $f'(\rho)/f(\rho) = -\rho/\sigma_x^2$  (white Gaussian host),  $K = 2p$  and  $\eta \sigma_x^2 = 2$ . The detection function is then

$$\begin{aligned} t(\mathbf{r}) &= k_t \left( (\sqrt{p} \mathbf{r}^T \mathbf{e}_p)^2 - \|\mathbf{r}\|^2 \right) \\ &= \frac{1}{\sigma_x^2 \sqrt{2p(p-1)}} \left( (p-1)r_p^2 - \sum_{i=1}^{p-1} r_i^2 \right) \end{aligned} \quad (36)$$

where  $t(\mathbf{r}) = \tau$  defines a  $p$ -dimensional two-sheet hyperboloid. This is closed to a two-sheet hypercone, acceptance region of the absolute normalized correlation, which is the optimum detection function based on such simple statistics for a Gaussian white host [3]. We agree here with Merhav and Sabbag that the acceptance region must be a two-sheet geometric form contrary to the well-known normalized correlation and its one-sheet hypercone [1]. Yet, neither the absolute normalized correlation nor the famous normalized correlation are fundamental solutions. We suppose that this stems from the difference in the models of the perceptual constraint: fixed embedding power versus random small and positive gain. Equation (36) is, however, not unknown

<sup>2</sup>Except on the boundaries due to discontinuities. This has little importance as the probability that the host signal is on a boundary is zero.

<sup>3</sup>The other solution  $\{t(r) = \sqrt{2} \sin(\sqrt{\eta}r), w(s) = \sqrt{2} \cos(\sqrt{\eta}s)\}$  is valid on a shifted partition  $\bigcup_i [(\pi/2\sqrt{\eta})(2i-1), (\pi/2\sqrt{\eta})(2i+1))$ .

in the watermarking literature. This is the measure of robustness given in Cox *et al.* book [1, Eq.(5.13)].

Let us now invent a host such that

$$P(\mathbf{s} \in \mathcal{B}_p(R)) = \begin{cases} \frac{R}{R_0}, & \text{if } R \leq R_0 \\ 1, & \text{if } R > R_0. \end{cases}$$

This extension of the one-dimension uniform distribution (in the sense that, in one dimension, a uniform distribution gives a linear cumulative distribution function over the interval  $\mathcal{B}_1(R)$ ) implies that its isotropic pdf is equal to  $f(\rho) = \rho^{1-p}/R_0$ , if  $0 < \rho < R_0$  (0, else). A solution in the form  $t(\mathbf{r}) = U(\rho)$  must then satisfy  $\eta U(\rho) + U''(\rho) = 0$ , whose solutions are as follows:

$$t^{(a)}(\rho) = \sqrt{2\text{surf}(\mathcal{S}_p(1))} \cos(\sqrt{\eta}\rho) \text{ with } \sqrt{\eta}R_0 = 0 [\pi] \quad (37)$$

$$t^{(b)}(\rho) = \sqrt{2\text{surf}(\mathcal{S}_p(1))} \sin(\sqrt{\eta}\rho) \text{ with } \sqrt{\eta}R_0 = 0 [2\pi] \quad (38)$$

where  $\text{surf}(\mathcal{S}_p(1))$  is the surface area of the  $p$ -hypersphere of unit radius  $\text{surf}(\mathcal{S}_p(1)) = 2\pi^{p/2}/\Gamma(p/2)$ . This solution looks similar to the sphere hardening dither modulation scheme invented by F. Balado [25, Sec. 5].

2) *Sparsity*: Many possible coordinate systems allow a separation of variables [24], but their investigation is out of the scope of this paper. Preferably, we would like here to rediscover a famous principle in watermarking. Suppose we know a solution  $t^*$  to the scalar equation  $\eta^* t^*(x) + f(x)t^{*\prime}(x) + t^{*\prime\prime}(x) = 0$ . We would like to extend this solution considering a solution in the form  $t = t^* \circ g$ , with  $g : \mathbb{R}^p \rightarrow \mathbb{R}$  a differentiable function. Gradient and Laplacian have the following expressions:

$$\begin{aligned} \nabla t(\mathbf{r}) &= t^{*\prime}(g(\mathbf{r}))\nabla g(\mathbf{r}) \\ \nabla^2 t(\mathbf{r}) &= t^{*\prime\prime}(g(\mathbf{r}))\|\nabla g(\mathbf{r})\|^2 + t^{*\prime}(g(\mathbf{r}))\nabla^2 g(\mathbf{r}) \end{aligned} \quad (39)$$

and the fundamental equation becomes

$$\begin{aligned} t^{*\prime}(g(\mathbf{r})) \left( -\frac{\eta}{\eta^*} f(g(\mathbf{r})) + \frac{\nabla p_{\mathbf{S}}(\mathbf{r})^T}{p_{\mathbf{S}}(\mathbf{r})} \nabla g(\mathbf{r}) + \nabla^2 g(\mathbf{r}) \right) \\ + t^{*\prime\prime}(g(\mathbf{r})) \left( \|\nabla g(\mathbf{r})\|^2 - \frac{\eta}{\eta^*} \right) = 0. \end{aligned} \quad (40)$$

A linear form, that is, a projection  $g(\mathbf{r}) = \mathbf{r}^T \boldsymbol{\lambda}$  is a solution providing the following simplifications:  $\nabla^2 g(\mathbf{r}) = 0$  and  $\|\nabla g(\mathbf{r})\| = \|\boldsymbol{\lambda}\|$ . Then,  $t$  is a fundamental solution with an efficiency per element  $\eta = \eta^* \|\boldsymbol{\lambda}\|^2$ , provided we have

$$\frac{\nabla p_{\mathbf{S}}(\mathbf{r})^T}{p_{\mathbf{S}}(\mathbf{r})} \boldsymbol{\lambda} = \|\boldsymbol{\lambda}\|^2 f(\mathbf{r}^T \boldsymbol{\lambda}). \quad (41)$$

For a white Gaussian host, this implies that  $f(x) = -x\|\boldsymbol{\lambda}\|^{-2}\sigma_x^{-2}$ , which is the score (i.e.,  $p'(x)/p(x)$ ) associated with  $\mathcal{N}(0, \|\boldsymbol{\lambda}\|^2\sigma_x^2)$ . Hence, the polynomial family is extended to the vector case with fundamental solutions of the form  $t_k(\mathbf{r}) = \kappa_k H_k(\mathbf{r}^T \boldsymbol{\lambda} / \|\boldsymbol{\lambda}\| \sigma_x)$  whose efficiency per element is  $\eta = k/\sigma_x^2$ .

For the flat host assumption,  $f$  appears to be the null function. Hence, the sinusoidal family is extended to the vector case with

the fundamental solution of the form  $t(\mathbf{r}) = k_t \cos(\mathbf{r}^T \boldsymbol{\lambda})$  whose efficacy is  $\eta = \|\boldsymbol{\lambda}\|^2$ .

This kind of solution illustrates the principle known as sparsity or time sharing [26, Secs. 5.2 and 8.2], where the watermark embedding is processed on the projection  $\mathbf{r}^T \boldsymbol{\lambda}$ . A typical implementation of this principle is the spread transform dither modulation [26, Sec. 5.2].

3) *Space Partitioning*: Under the flat host assumption, (25) is reduced to the well-known Helmholtz equation  $\eta t(\mathbf{r}) + \nabla^2 t(\mathbf{r}) = 0$ . Suppose  $t^*$  is a solution, then the composition of this function by a translation operator yields another solution  $t_0(\mathbf{r}) = t^*(\mathbf{r} - \mathbf{r}_0)$ . This property is due to the fact that the score  $\nabla p_{\mathbf{S}}(\mathbf{r})/p_{\mathbf{S}}(\mathbf{r})$  is invariant by translation since it is null. One can also mix different solutions defined over a specific region  $\mathcal{C}_i \subset \mathbb{R}^p t(\mathbf{r}) = \sum_i t_i(\mathbf{r}) \Pi_i(\mathbf{r})$ , with  $\Pi_i(\cdot)$  the indicator function of region  $\mathcal{C}_i$ . Assume now that regions  $\{\mathcal{C}_i\}$  constitute a partition of  $\mathbb{R}^p$  and that the host pdf is a piecewise constant function such that  $p_{\mathbf{S}}(\mathbf{s}) = \sum_i P_i \Pi_i(\mathbf{s})$ . Then, the above mixture is a solution of the fundamental equation, except on the boundaries of contiguous regions where the gradients of  $p_{\mathbf{S}}$  and  $t$  are *a priori* not defined.

An elegant way to set a partition is to define the regions as the Voronoi cells of a  $p$ -dimension lattice  $\Lambda: \mathcal{C}_i = \mathcal{V} + \mathbf{c}_i$ ,  $\mathbf{c}_i \in \Lambda$  and  $\mathcal{V}$  the Voronoi cell centered on  $\mathbf{0}$ . With all of these elements, we can write

$$t(\mathbf{r}) = \sum_i t_i(\mathbf{r}) \Pi_i(\mathbf{r}) = \sum_{\mathbf{c}_i \in \Lambda} t^*(\mathbf{r} - \mathbf{c}_i) \Pi_i(\mathbf{r}) = t^*(\mathbf{r} - Q(\mathbf{r})) \quad (42)$$

with  $Q(\cdot)$  the quantization function mapping  $\mathbb{R}^p$  onto  $\Lambda$ .

Under the flat host assumption, sparsity and space partitioning indeed give the same extension of the sinusoidal family  $t_{\mathbf{k}}(\mathbf{r}) = \sqrt{2} \cos(\mathbf{r}^T \boldsymbol{\lambda}_{\mathbf{k}})$ , when vector  $\boldsymbol{\lambda}_{\mathbf{k}}$  is defined by  $2\pi G^{-T} \mathbf{k}$ , with  $G$  the generator matrix of lattice  $\Lambda$  and  $\mathbf{k} \in \mathbb{N}^p$ .  $\mathbf{r}$  belonging to  $\mathcal{C}_i$  means that  $\mathbf{r} = \mathbf{c}_i + \tilde{\mathbf{r}} = G\mathbf{n}_i + \tilde{\mathbf{r}}$ , with  $\mathbf{n}_i \in \mathbb{Z}^p$  and  $\tilde{\mathbf{r}} \in \mathcal{V}$ . Thus,  $t(\mathbf{r}) = t(\tilde{\mathbf{r}})$  because  $\mathbf{n}_i^T \mathbf{k} \in \mathbb{Z}$ ,  $\forall(\mathbf{k}, \mathbf{n}_i) \in \mathbb{N}^p \times \mathbb{Z}^p$ . This gives  $\eta = \|\boldsymbol{\lambda}_{\mathbf{k}}\|^2 = 4\pi^2 \|G^{-T} \mathbf{k}\|^2$ . Once again, this is not exactly the lattice quantizer-based watermarking scheme, but at least we find back solutions which are periodic with respect to a lattice.

To conclude, the goal of this section is to show that several well-known watermarking schemes are indeed solutions of the fundamental equation, underlying the unifying character of this theoretical framework.

## V. CONDITIONS, LIMITATIONS, AND EXTENSIONS

### A. Conditions

Many assumptions have been made to derive the fundamental equation and we would like to collect and state them explicitly in this section before providing some limitations and extensions.

First, at the embedding side, the model of the perceptual constraint is based on the masking phenomenon, modeled as a perceptual gain  $\theta$ . Whereas this article focuses on a scalar gain for sake of simplicity, in practice, it is likely to be a vector of positive and small values locally adapting the power of the watermark signal to the power of the masking effect. The main fact

is that this gain is unknown when generating the energy constrained signal  $\mathbf{w}(\mathbf{s})$ , and unknown at the detection side. This model is quite different than the classical power or energy constraint, which imposes a fixed amount of embedding distortion.

Second, in this paper, schemes are claimed optimal if they maximize the efficiency per sample. This meaning of optimality only holds when the Pitman–Noether theorem can be applied (i.e., for schemes fulfilling the following regularity assumptions) [11, Sec. III-C3].

- The energy of the watermark signal and the variance of the tested statistic must be bounded. Without loss of generality, we impose  $E_{\mathbf{S}}\{\|\mathbf{w}(\mathbf{s})\|^2\} = n$  and  $E_{\mathbf{R}}\{t(\mathbf{r})^2\} = 1$ .
- The smoothness conditions on the density  $p(\cdot|\mathcal{H}_1)$  as a function of  $\theta$  and on the nonlinearity  $t(\cdot)$  such that (5) holds.
- The convergence in law of the statistic  $t(\mathbf{R})$  to a normal variable under both hypotheses.

Moreover, we also restrict our study to detection functions defined in  $\mathbb{R}^n$  at least twice differentiable except on a zero-measure set to obtain the existence of its gradient and Laplacian. Then, the above study can be summarized in the following proposition.

*Proposition 1:* Suppose a zero-bit watermarking scheme based on the embedding and detection functions  $\{\mathbf{w}(\cdot), t(\cdot)\}$  satisfies the previously mentioned conditions. Then, this scheme is optimal for a given efficacy  $\eta$  and when there is no attack, if and only if  $t(\cdot)$  is a solution of the fundamental (24) and  $w(\mathbf{s}) = k_w \nabla t(\mathbf{s})$ ,  $\forall \mathbf{s} \in \mathbb{R}^n$ .

The convergence in law to a normal variable is a very restrictive condition. When the host samples are i.i.d. (or blocked based i.i.d.), block-based embedding gives an elegant solution because its matched detection function is the sum of  $n/p$  i.i.d. random variables. The parameter  $p$  must be fixed to ensure the asymptotic normality by the central limit theorem (as  $E\{t^{(p)}(\mathbf{r})^2\} < +\infty$ ).

*Proposition 2:* The principle of block-based embedding gives birth to two important families of detection functions: sums of  $p$ -multivariate Hermite polynomials for white Gaussian hosts, and sums of cosine functions periodically defined on  $p$ -dimension lattices for flat hosts. Both families gather orthonormal functions for the scalar product defined by (26).

## B. Limitations

The Pitman–Noether theorem states that the efficacy is a criterion for optimality only asymptotically. This makes sense in our study because the watermark signal is deeply embedded in the host, thus requiring spreading of the mark on long sequences. In the same way, efficacy is very useful in applications, such as passive sonar and radio astronomy, also dealing with weak signals and long integration times.

Our framework nicely gives a unified theory, gathering many known watermarking schemes. However, all new fundamental solutions may not be adequate for practical implementations where host signals are not so long, or  $\theta$  is not so small. We foresee at least two reasons.

- 1) When  $\theta$  is not so small, the variance under  $\mathcal{H}_1$  grows very fast with the efficacy, as shown in Appendix B and in Table I.

- 2) The Berry–Esseen theorem shows that the rate of convergence to the normal distribution depends on the third moment of  $t(\cdot)$ , which we suspect to be fast increasing with the efficacy.

A proper study requires a nonasymptotic analysis of the performances which is out of the scope of this article. Some experimental works can be found in the literature. For instance, the  $p$ -multivariate Hermite polynomial-based family of detection functions has been already experimentally tested under the abbreviation JANIS: in [17], the efficacy is given by the order of the JANIS scheme (i.e.,  $\eta = p$ ). The receiver operating characteristic (ROC) curve [i.e.,  $P_p = P_p(P_{fa})$  for a given embedding gain] and the “power” curve (i.e.,  $P_p = P_p(\theta)$  for a given  $P_{fa}$ ) are largely improved compared to performances of spread-spectrum (SS) watermarking scheme (see, respectively, [17, Figs. 3 and 4]). However, for a given vector length, the comparison of the performances based on a normal distribution of the tested statistic with the experimental measurements clearly mismatch as the efficacy increases and as the parameter  $\theta$  increases. Hence, whereas the central limit theorem proves the asymptotic convergence in law needed in the theoretical framework, in any case, it shall not be used to estimate performances in practice. Another lesson learned from [17] is that a scheme with higher efficacy can perform more poorly than another one in a nonasymptotic regime. In [17, Fig. 3], the scheme with  $p = 5$  yields higher power than the one with  $p = 4$  only if  $P_{fa} > 10^{-3}$ , with  $n = 2400$  for both schemes.

Whereas this study provides a somewhat elegant, constructive, and unifying theoretical framework, unfortunately, it does not provide clear guidelines on the design of a watermarking scheme in a nonasymptotic regime.

## C. Extension to Asymmetric Tests

So far, the main idea of this paper is to take advantage of the knowledge of the host value  $\mathbf{s}$  to boost the efficiency per element. This results in an increase of  $E_{\mathbf{R}}\{t(\mathbf{r})|\mathcal{H}_1\} = \theta\sqrt{n\eta} + O(\theta^2)$ , while the variance  $\text{Var}\{t(\mathbf{r})|\mathcal{H}_1\}$  is maintained at the level of  $\text{Var}\{t(\mathbf{r})|\mathcal{H}_0\}$  at least to the first order. Asymptotically, the test has to make a clear cut between two distributions having the same variance. This is sometimes called a symmetric test. This subsection focuses on the variance  $\text{Var}(t(\mathbf{r})|\mathcal{H}_1)$ . As Malvar and Florencio did for zero-rate watermarking [27], we would like to control the value of  $\text{Var}(t(\mathbf{r})|\mathcal{H}_1)$ , achieving so-called asymmetric tests.<sup>4</sup>

The watermark signal is already dependent to the host through the vector  $\mathbf{w}(\mathbf{s})$  which pushes the host toward a region in space where the detection function has a higher value (i.e., hopefully the acceptance region). We add here another dependence which modulates the amplitude of this vector: host signals which are naturally far away from the acceptance region are more strongly pushed than those near the acceptance region. We write the watermark signal  $\mathbf{x}(\mathbf{s}) = \theta k_w(\mathbf{s})\mathbf{w}(\mathbf{s})$ . For a fair comparison with the previous sections, the constraint

<sup>4</sup>Be careful not to confuse this with asymmetric watermarking where the detection key is different from the embedding private key.

reads  $\mathbb{E}_{\mathbf{S}}\{k_w(\mathbf{s})^2\|\mathbf{w}(\mathbf{s})\|^2\} = n$ . The embedding strategy is not changed  $\mathbf{w}(\mathbf{s}) = \nabla t(\mathbf{s})$ . Hence, we have

$$n = \mathbb{E}_{\mathbf{S}}\{k_w(\mathbf{s})^2\|\nabla t(\mathbf{s})\|^2\} \quad (43)$$

$$\left. \frac{\partial}{\partial \theta} \mathbb{E}_{\mathbf{R}}\{t(\mathbf{r})|\mathcal{H}_1\} \right|_{\theta=0} = \mathbb{E}_{\mathbf{S}}\{k_w(\mathbf{s})\|\nabla t(\mathbf{s})\|^2\} \quad (44)$$

$$\eta = \frac{\mathbb{E}_{\mathbf{S}}\{k_w(\mathbf{s})\|\nabla t(\mathbf{s})\|^2\}^2}{\mathbb{E}_{\mathbf{S}}\{k_w(\mathbf{s})^2\|\nabla t(\mathbf{s})\|^2\}}. \quad (45)$$

Now, the goal is to choose function  $k_w$  such that it reduces the variance under  $\mathcal{H}_1$

$$\left. \frac{\partial}{\partial \theta} \text{Var}\{t(\mathbf{r})|\mathcal{H}_1\} \right|_{\theta=0} = 2\mathbb{E}_{\mathbf{S}}\{t(\mathbf{s})\tilde{\nu}(\mathbf{s})\} \geq -2\text{Var}\{\nu(\mathbf{s})\} \quad (46)$$

where  $\nu(\mathbf{s}) = k_w(\mathbf{s})\|\nabla t(\mathbf{s})\|^2$  such that its centered version is  $\tilde{\nu}(\mathbf{s}) = \nu(\mathbf{s}) - (\partial/\partial\theta)\mathbb{E}_{\mathbf{R}}\{t(\mathbf{r})|\mathcal{H}_1\}|_{\theta=0}$ . The Cauchy–Schwarz inequality gives  $-2\text{Var}\{\nu(\mathbf{s})\}$  as the lower-bound, with equality when  $\tilde{\nu}(\mathbf{s}) = -c t(\mathbf{s})$ ,  $c$  a positive constant. Hence, we succeed in reducing  $\text{Var}\{t(\mathbf{r})|\mathcal{H}_1\}$ . However, this strategy consumes embedding distortion

$$\begin{aligned} n &= \mathbb{E}_{\mathbf{S}}\{k_w(\mathbf{s})^2\|\nabla t(\mathbf{s})\|^2\} = \mathbb{E}_{\mathbf{S}}\{\nu(\mathbf{s})^2\|\nabla t(\mathbf{s})\|^{-2}\} \\ &= c^2\mathbb{E}_{\mathbf{S}}\{t(\mathbf{s})^2\|\nabla t(\mathbf{s})\|^{-2}\} + n\eta\mathbb{E}_{\mathbf{S}}\{\|\nabla t(\mathbf{s})\|^{-2}\} \\ &\quad - 2c\sqrt{n\eta}\mathbb{E}_{\mathbf{S}}\{t(\mathbf{s})\|\nabla t(\mathbf{s})\|^{-2}\}. \end{aligned} \quad (47)$$

For the simple cases explored in this paper, we are able to find a bijection  $\mathbf{s}' = h(\mathbf{s})$  such that  $p_{\mathbf{S}}(\mathbf{s}')t(\mathbf{s}')\|\nabla t(\mathbf{s}')\|^{-2} = -p_{\mathbf{S}}(\mathbf{s})t(\mathbf{s})\|\nabla t(\mathbf{s})\|^{-2}$ , which implies a third null term. Denote  $a = \mathbb{E}_{\mathbf{S}}\{t(\mathbf{s})^2\|\nabla t(\mathbf{s})\|^{-2}\}$  and  $b = \mathbb{E}_{\mathbf{S}}\{\|\nabla t(\mathbf{s})\|^{-2}\}$ . Equation (47) finally reads

$$n = ac^2 + bn\eta. \quad (48)$$

A higher  $c$  decreases  $\text{Var}\{t(\mathbf{r})|\mathcal{H}_1\}$  (first-order approximation) but also  $\eta$  due to the distortion constraint. In practice, this strategy presents a crucial issue. Starting from a tested statistic having a symmetric distribution under both hypotheses, a decrease of  $\text{Var}\{t(\mathbf{r})|\mathcal{H}_1\}$  yields a higher power of test only if  $\mathbb{E}_{\mathbf{R}}\{t(\mathbf{r})|\mathcal{H}_1\}$  is greater than threshold  $\tau > 0$ . Now, if this is not the case (for instance, due to an attack), then the impact of this strategy is just the opposite. This phenomenon does not appear in [27] as this article tackles watermark decoding where threshold  $\tau$  is equal to 0, the distributions under  $\mathcal{H}_0$  (bit 1 has been hidden) and  $\mathcal{H}_1$  (bit 0 has been hidden) are symmetric around this value.

Experimental work about this variance reducing embedding strategy applied to the JANIS scheme is summarized in [5, Sec. 6.4]. It stresses the difficulty in finding an appropriate value of  $c$  because it requires foreseeing an attack scenario and its impact on the expectation of the tested statistic. The final rule applied in this experimental paper is to set  $c$  to the value which maximizes the Gaussian estimation of the power of test (which is, once again, a very poor estimation). Results are mitigated and more complex embedding strategies are investigated in [5, Sec. 6.4].

## VI. ATTACK NOISE

When there is an attack, the received signal under  $\mathcal{H}_1$  is  $\mathbf{r}_1 = \mathbf{a}(\mathbf{y})$ . The attack channel  $\mathbf{a}$  is defined through a conditional probability distribution  $p_a(\mathbf{r}_1|\mathbf{y})$ , whose associated attack power is  $\sigma_a^2 = \int \int \|\mathbf{r}_1 - \mathbf{y}\|^2 p_a(\mathbf{r}_1|\mathbf{y}) p_{\mathbf{Y}}(\mathbf{y}) d\mathbf{y} d\mathbf{r}_1 / n$ . The parameters of the attack channel are unknown at the detection side. We would like to keep the detection as simple as possible so that the estimation of these parameters is not tractable in this strategy. The performance of the detector should degrade slowly with the strength of the attack, according to the definition of robust watermarking given in [28].

The Pitman–Noether theorem might then become useless because there is a disruption between the two hypotheses.  $\mathcal{H}_1$  does not asymptotically converge to  $\mathcal{H}_0$  in the sense that the regularity conditions (5) are violated due to the presence of the attack channel under only  $\mathcal{H}_1$ .

Here, we present two ways to tackle this problem, changing our framework in order to enforce the Pitman–Noether theorem. The first idea is to restrict our analysis to a fixed watermark-to-noise-power ratio (WNR):  $\theta_n^2/\sigma_a^2 = g$ . The received signal can be written as  $\mathbf{r}_1 = \mathbf{s} + \theta_n \mathbf{w}(\mathbf{s}) + \theta_n g^{-1/2} \tilde{\mathbf{z}}$ , with  $\mathbb{E}_{\mathbf{Z}}\{\|\tilde{\mathbf{z}}\|^2\} = n$ . Therefore, the power of the difference signal  $\mathbf{r}_1 - \mathbf{r}_0$  asymptotically vanishes with  $\theta_n^2$ . The second idea considers attacks with fixed DNR (document, that is, host, to noise power ratio) where signals are corrupted by the same attack under both hypotheses as Liu and Moulin accomplished [6]. Yet, the targeted applications as described in our introduction do not *a priori* motivate this possibility because the attack of unprotected contents under  $\mathcal{H}_0$  are clearly unlikely. We argue that a “soft” attack on original pieces of content still produces regular content. The attack channel changes the value of the feature vectors, but it does not modify their inherent statistical structure.

Under both attack models, the fundamental equation appears to be statistically robust in the sense that it is not modified by the presence of the attack channel. However, this is only true for very particular conditions as described in the sequel.

### A. Fixed WNR Attacks

This subsection only shows that the fundamental equation remains unchanged when the watermarked signals go through a fixed WNR AWGN attack channel.

1) *Best Embedding Function for a Given Detection Function:* As usual, we write

$$\begin{aligned} &\left. \frac{\partial}{\partial \theta} \mathbb{E}_{\mathbf{R}}\{t(\mathbf{r})|\mathcal{H}_1\} \right|_{\theta=0} \\ &= \int \int \frac{\partial}{\partial \theta} t(\mathbf{s} + \theta \mathbf{w}(\mathbf{s}) + \theta \sqrt{g} \tilde{\mathbf{z}}) \Big|_{\theta=0} p_{\mathbf{S}}(\mathbf{s}) p_{\tilde{\mathbf{Z}}}(\tilde{\mathbf{z}}) d\mathbf{s} d\tilde{\mathbf{z}} \\ &= \int \mathbf{w}(\mathbf{s})^T \nabla t(\mathbf{s}) p_{\mathbf{S}}(\mathbf{s}) d\mathbf{s} \\ &\quad + \int \int \sqrt{g} \tilde{\mathbf{z}}^T \nabla t(\mathbf{s}) p_{\mathbf{S}}(\mathbf{s}) p_{\tilde{\mathbf{Z}}}(\tilde{\mathbf{z}}) d\mathbf{s} d\tilde{\mathbf{z}}. \end{aligned}$$

We assume  $\tilde{\mathbf{z}}$  is independent of  $\mathbf{s}$  and centered, so that the second term is null. We find back the same best embedder as (21).

2) *Best Detection Function for a Given Embedding Function:* The pdf of  $\mathbf{r}_1 = \mathbf{y} + \sqrt{g\theta}\tilde{\mathbf{z}}$  is given by the following convolution:

$$p_{\mathbf{R}_1}(\mathbf{r}) = \int p_{\mathbf{Y}}(\mathbf{u})p_{\sqrt{g\theta}\tilde{\mathbf{z}}}(\mathbf{r} - \mathbf{u})d\mathbf{u} \quad (49)$$

whose derivative is composed of two terms

$$\begin{aligned} \frac{\partial}{\partial\theta}p_{\mathbf{R}_1}(\mathbf{r})\Big|_{\theta=0} &= \int \frac{\partial}{\partial\theta}p_{\mathbf{Y}}(\mathbf{u})\Big|_{\theta=0} \lim_{\theta \rightarrow 0} p_{\sqrt{g\theta}\tilde{\mathbf{z}}}(\mathbf{r} - \mathbf{u})d\mathbf{u} \\ &+ \int p_{\mathbf{S}}(\mathbf{u}) \frac{\partial}{\partial\theta}p_{\sqrt{g\theta}\tilde{\mathbf{z}}}(\mathbf{r} - \mathbf{u})\Big|_{\theta=0} d\mathbf{u}. \end{aligned} \quad (50)$$

We assume that  $\tilde{\mathbf{z}}$  is normal distributed. Then,  $\lim_{\theta \rightarrow 0} p_{\sqrt{g\theta}\tilde{\mathbf{z}}}(\mathbf{r} - \mathbf{u})$  is the Dirac distribution. Hence, the first term is, as detailed in Section III-A,  $\partial/\partial\theta p_{\mathbf{Y}}(\mathbf{r})\Big|_{\theta=0} = -\text{div}(p_{\mathbf{S}}(\mathbf{r})\mathbf{w}(\mathbf{r}))$ .

The second term is calculated as being inspired by some proofs of the De Bruijn's identity (see [29, Th. 16.6.2]). It corresponds to the derivative of the pdf of  $\mathbf{a}(\mathbf{s}) = \mathbf{s} + \sqrt{g\theta}\tilde{\mathbf{z}}$  with respect to  $\theta$ . On one hand, we have

$$\frac{\partial}{\partial\theta}p_{\mathbf{a}(\mathbf{s})}(\mathbf{r}) = \int p_{\mathbf{S}}(\mathbf{u}) \left( \frac{\|\mathbf{r} - \mathbf{u}\|^2}{g\theta^3} - \frac{n}{\theta} \right) p_{\sqrt{g\theta}\tilde{\mathbf{z}}}(\mathbf{r} - \mathbf{u})d\mathbf{u}. \quad (51)$$

On the other hand, it appears that

$$\begin{aligned} \nabla^2 p_{\mathbf{a}(\mathbf{s})}(\mathbf{r}) &= \int p_{\mathbf{S}}(\mathbf{u}) \left( \frac{\|\mathbf{r} - \mathbf{u}\|^2}{g^2\theta^4} - \frac{n}{g\theta^2} \right) p_{\sqrt{g\theta}\tilde{\mathbf{z}}}(\mathbf{r} - \mathbf{u})d\mathbf{u} \\ &= \frac{1}{g\theta} \frac{\partial}{\partial\theta} p_{\mathbf{a}(\mathbf{s})}(\mathbf{r}). \end{aligned} \quad (52)$$

Finally, the second term is null, because

$$\frac{\partial}{\partial\theta}p_{\mathbf{a}(\mathbf{s})}(\mathbf{r})\Big|_{\theta=0} = \lim_{\theta \rightarrow 0} g\theta \nabla^2 p_{\mathbf{a}(\mathbf{s})}(\mathbf{r}) = 0 \quad (53)$$

and we find the same best detection function as (13).

### B. Fixed DNR Attacks

The framework is changed so that the hypotheses are now  $\mathcal{H}_0 : \mathbf{r}_0 = \mathbf{a}(\mathbf{s})$  against  $\mathcal{H}_1 : \mathbf{r}_1 = \mathbf{a}(\mathbf{s} + \theta\mathbf{w}(\mathbf{s}))$ . What are the impacts of this new framework on the detection and embedding functions?

As already stated, our analysis only holds for channel attacks conserving the statistical structure of the host signal. The restrictions are as follows. For host  $\mathbf{s} \sim \mathcal{N}(\mathbf{0}, \mathbf{I}_n)$ , the attack is a scaling and additive white Gaussian noise (SAWGN) channel  $\mathbf{a}(\mathbf{s}) = \gamma(\mathbf{s} + \mathbf{z})$ , with  $\mathbf{z} \sim \mathcal{N}(\mathbf{0}, \sigma_z^2 \mathbf{I}_n)$  independent of  $\mathbf{s}$  and  $\gamma = 1/\sqrt{1 + \sigma_z^2}$ . The attack is Wiener filtering for this very simple case, which maintains  $p(\mathbf{r}|\mathcal{H}_0)$  as a normal distribution. For the flat host assumption, the attack is the addition of independent noise  $\mathbf{a}(\mathbf{s}) = \mathbf{s} + \mathbf{z}$ . The new expression of  $p(\mathbf{r}|\mathcal{H}_0)$  is given by a convolution, which renders the pdf under  $\mathcal{H}_0$  to be even flatter and larger. Consequently, at the scale of the watermarking signal,  $p(\mathbf{r}|\mathcal{H}_0)$  is still a piecewise constant function. The expression (12) of the best detection function with the embedding function is not modified when restricted to attack channels preserving  $p(\mathbf{r}|\mathcal{H}_0)$ .

This is not the case for the best embedding function given the detection function. For the class of attack channel considered

in this paper, we can write  $\mathbf{a}(\mathbf{s}) = \gamma(\mathbf{s} + \mathbf{z})$  with  $\gamma = 1$  for the additive noise attack, and  $\gamma = 1/\sqrt{1 + \sigma_z^2}$  for the SAWGN attack. Equation (19) is then modified as follows:

$$\begin{aligned} \frac{\partial}{\partial\theta} E_{\mathbf{R}}\{t(\mathbf{r})|\mathcal{H}_1\}\Big|_{\theta=0}(\gamma, \sigma_z) &= \int \int \frac{\partial}{\partial\theta} t(\gamma(\mathbf{s} + \theta\mathbf{w}(\mathbf{s}) + \mathbf{z}))\Big|_{\theta=0} p_{\mathbf{Z}}(\mathbf{z})p_{\mathbf{S}}(\mathbf{s})d\mathbf{z}d\mathbf{s} \\ &= \int \gamma\mathbf{w}(\mathbf{s})^T \left( \int \nabla t(\gamma(\mathbf{s} + \mathbf{z}))p_{\mathbf{Z}}(\mathbf{z})d\mathbf{z} \right) p_{\mathbf{S}}(\mathbf{s})d\mathbf{s}. \end{aligned} \quad (54)$$

This last equation shows that the best strategy at the embedding side should set

$$\mathbf{w}(\mathbf{s}) \propto E_{\mathbf{Z}}\{\nabla t(\gamma(\mathbf{s} + \mathbf{z}))\}. \quad (55)$$

This implies that the embedder knows the attack channel parameters. This counterattack may not be realistic in general, and we keep our former strategy given by (21), so that

$$\eta(\gamma, \sigma_z) = \frac{\gamma^2 \eta(1, 0)}{n^2} (E_{\mathbf{S}}\{\mathbf{w}(\mathbf{s})^T E_{\mathbf{Z}}\{\mathbf{w}(\gamma(\mathbf{s} + \mathbf{z}))\}\})^2. \quad (56)$$

However, there are some cases where the counterattack (55) is surprisingly simple because it is indeed identical to the regular embedding strategy (21) regardless of the parameters of the attack channel. This occurs when  $t$  is such that  $E_{\mathbf{Z}}\{\nabla t(\gamma(\mathbf{s} + \mathbf{z}))\} = h(\gamma, \sigma_z)\nabla t(\mathbf{s})$ . As a consequence, the fundamental equation (25) derived in the no-attack case, remains valid under these particular attack cases. The efficiency per element is then equal to  $\eta(\gamma, \sigma_z) = \gamma^2 h^2(\gamma, \sigma_z)\eta(1, 0)$ .

For the polynomial family, we rewrite Wiener filtering, denoting  $\tilde{z} = \sigma_z^{-1}z$  distributed as  $\mathcal{N}(0, 1)$  and  $\alpha = \arccos(\gamma)$ . A less familiar identity of the Hermite polynomials will allow one to write

$$\begin{aligned} t'_\ell(\gamma(\mathbf{s} + \mathbf{z})) &= \kappa_{\ell} \ell H_{\ell-1}(\cos(\alpha)\mathbf{s} + \sin(\alpha)\tilde{\mathbf{z}}) \\ &= \kappa_{\ell} \ell \sum_{k=0}^{\ell-1} \binom{\ell-1}{k} \cos^k(\alpha) \sin^{\ell-1-k}(\alpha) H_k(\mathbf{s}) H_{\ell-1-k}(\tilde{\mathbf{z}}). \end{aligned} \quad (57)$$

$E_{\mathbf{Z}}\{t'_\ell(\gamma(\mathbf{s} + \mathbf{z}))\}$  reduces to  $E_{\tilde{\mathbf{Z}}}\{t'_\ell(\gamma\mathbf{s} + \sigma_z\tilde{\mathbf{z}})\} = \kappa_{\ell} \ell \gamma^{\ell-1} H_{\ell-1}(\mathbf{s}) = \gamma^{\ell-1} t'_\ell(\mathbf{s})$  because  $E_{\tilde{\mathbf{Z}}}\{H_k(\tilde{\mathbf{z}})\} = \delta(k)$ . Consequently, we can state the following proposition:

*Proposition 3:* The polynomial family is a set of fundamental solutions for i.i.d. Gaussian hosts and SAWGN attacks with Wiener filtering, whose efficiency per element is given by  $\eta(\gamma, \sigma_z) = \ell \gamma^{2\ell}$ . Wiener filtering means that  $\gamma = (1 + \sigma_z^2)^{-1/2}$ .

Two noticeable exemptions are  $t_1$  and  $t_2$ , whose efficiency follows the same rule whatever the value of  $\gamma$  in the SAWGN channel is. Last but not least, the higher the "original" efficiency  $\eta(1, 0) = \ell$  is, the less robust is the scheme in the sense that  $\eta(\gamma, \sigma_z)/\eta(1, 0) = (1 + \sigma_z^2)^{-\eta(1, 0)}$  decreases faster with the strength of the attack.

For the sinusoidal family, additive noise leads to

$$\begin{aligned} E_{\mathbf{Z}}\{t'_\ell(\mathbf{s} + \mathbf{z})\} &= t'_\ell(\mathbf{s})E_{\mathbf{Z}}\{\cos(\ell\sqrt{\eta}\mathbf{z})\} \\ &= \ell\sqrt{2\eta} \cos(\ell\sqrt{\eta}\mathbf{s})E_{\mathbf{Z}}\{\sin(\ell\sqrt{\eta}\mathbf{z})\}. \end{aligned} \quad (58)$$

The desired property is enabled whenever the attack noise has an even pdf which sets the second term to zero. For instance, the AWGN channel gives  $\mathbb{E}_Z\{t'_\ell(s+z)\} = t'_\ell(s)e^{-\ell\sqrt{\eta}\sigma_z^2/2}$ . Consequently, we can state the following proposition:

*Proposition 4:* The sinusoidal family is a set of fundamental solutions for flat hosts and additive symmetric noise attacks. For the AWGN channel attack, its efficiency is given by  $\eta(1, \sigma_z) = \ell\sqrt{\eta}e^{-\ell\sqrt{\eta}\sigma_z^2}$ .

Once again, the higher the “original” efficiency  $\eta(1, 0)$  is, the less robust the scheme is in the sense that  $\eta(\gamma, \sigma_z)/\eta(1, 0) = e^{-\eta(1,0)\sigma_z^2}$  decreases faster with the strength of the attack.

The same analysis also holds for the extension of the polynomial and sinusoidal family to the vector case. For instance, JANIS is a solution of the fundamental equation for i.i.d. hosts and SAWGN attack, such that  $\mathbb{E}_Z\{\nabla t(\gamma(\mathbf{s} + \mathbf{z}))\} = \gamma^{p-1}\nabla t(\mathbf{s})$ . The Wiener filtering restriction is not necessary as JANIS is based on first-order Hermite polynomials. This gives the following efficiency per element  $\eta(\gamma, \sigma_z) = p\gamma^{2p}$  which follows the same decreasing rule as the scalar polynomial family. The extended sinusoidal family follows the same rule  $\eta(1, \sigma_z)/\eta(1, 0) = e^{-\eta(1,0)\sigma_z^2}$  with  $\eta(1, 0) = 4\pi^2\|G^{-T}\mathbf{k}\|^2$  as shown in Appendix C.

## VII. ABOUT DC-DM WATERMARKING BASED ON LATTICE QUANTIZATION

Our theoretical framework does not succeed in rediscovering well-known DC-DM watermarking schemes based on lattice quantization, where the detection function is usually defined by Euclidean distance  $t(\mathbf{r}) = k_t\|Q(\mathbf{r}) - \mathbf{r}\|^2$ , and the embedding function  $\mathbf{x}(\mathbf{s}) = \alpha(Q(\mathbf{s}) - \mathbf{s})$  complies with rule (21). Parameter  $\alpha$  is fixed and it plays a crucial role in the tradeoff between the embedding distortion and the inherent robustness of the scheme. Note that our point of view is very different as we assume that the host signal is pushed in a direction given by  $\mathbf{w}(\mathbf{s}) = k_t\nabla t(\mathbf{s}) = 2k_t(Q(\mathbf{s}) - \mathbf{s})$ , but the watermark signal  $\mathbf{x}(\mathbf{s}) = \theta\mathbf{w}(\mathbf{s})$  is not deterministic because the amplitude  $\theta$  is not fixed.

### A. Efficiency Without Noise

We consider a lattice  $\Lambda$  and a host whose pdf is a piecewise constant function over the partition induced by  $\Lambda$ :  $\mathbb{R}^p = \bigcup_{\mathbf{c}_i \in \Lambda} (\mathcal{V} + \mathbf{c}_i)$ . We study the detection function given by  $t(\mathbf{r}) = k_t(\|Q(\mathbf{r}) - \mathbf{r}\|^2 - \mu)$ , with  $Q$  being the quantizer associated with  $\Lambda$ , and  $\{k_t, \mu\}$  enforcing a centered unit variance tested statistic under  $\mathcal{H}_0$

$$\mu = \text{vol}(\mathcal{V})^{-1} \int_{\mathcal{V}} \|\mathbf{r}\|^2 d\mathbf{r} = I(\Lambda, 2) \quad (59)$$

$$\begin{aligned} k_t &= - \left( \text{vol}(\mathcal{V})^{-1} \int_{\mathcal{V}} \|\mathbf{r}\|^4 d\mathbf{r} - \mu^2 \right)^{-1/2} \\ &= - (I(\Lambda, 4) - I(\Lambda, 2)^2)^{-1/2}. \end{aligned} \quad (60)$$

$I(\Lambda, k)$  denotes the  $k$ th normalized moment of  $\mathcal{V}$  (i.e.,  $\text{vol}(\mathcal{V})^{-1} \int_{\mathcal{V}} \|\mathbf{r}\|^k d\mathbf{r}$ ). The embedding function is  $\mathbf{w}(\mathbf{s}) =$

$2k_w k_t (Q(\mathbf{r}) - \mathbf{r})$  (i.e., a vector pointing toward the nearest element of the lattice). Constant  $k_w$  is given by

$$k_w = \frac{\sqrt{n}}{2k_t \sqrt{I(\Lambda, 2)}}. \quad (61)$$

Finally, (23) gives the following efficiency per element for the noiseless case:

$$\eta = \frac{4I(\Lambda, 2)}{I(\Lambda, 4) - I(\Lambda, 2)^2}. \quad (62)$$

For a positive scale factor  $\beta < 1$  giving a finer partition induced by  $\beta\Lambda$ , we have a higher efficiency  $\eta_{\beta\Lambda} = \beta^{-2}\eta_\Lambda$ . Therefore, lattices should be compared for partitions with  $\text{vol}(\mathcal{V}) = 1$ . Anyways, finding the optimal lattice giving the best efficiency is out of the scope of this paper. As an example, for cubic lattice  $\Lambda = \mathbb{Z}^p$ ,  $\mathcal{V}$  is the centered hypercube  $[-1/2, 1/2]^p$  and  $\eta = 60$ . For the two-dimension hexagonal lattice  $A_2$ , whose associated generating matrix is  $G = [21; 0\sqrt{3}]/\sqrt{2\sqrt{3}}$  such that  $\text{vol}(\mathcal{V}) = 1$ , we achieve a higher efficiency per element  $\eta = 1800\sqrt{3}/43 \approx 72.50$ . Compared to the square lattice  $\mathbb{Z}^2$ , the “more spherical” of the two lattices is the best, when no attack is considered. This is surprisingly different from the zero-rate case presented in [21, Sec. 3.3].

Increasing the integer  $p$ , lattices exist with a nearly spherical Voronoi cell. Assuming  $\mathcal{V} = \mathcal{B}_p(R)$ , the efficiency reads  $\eta = (p+4)(p+2)R^{-2}$ . Setting  $R = \Gamma(p/2 + 1)^{1/p}/\sqrt{\pi}$  such that  $\text{vol}(\mathcal{V}) = 1$ , and using Stirling’s approximation, we achieve a linear efficiency per element  $\eta \approx 2\pi ep$ . In view of Section V-B, the issue is now whether we can increase parameter  $p$ , which is the size of the blocks. The tested statistic reads in terms of the square norm of a quantization noise of a flat host, which is not asymptotically Gaussian. Once again, we are facing the limitations of the Pitman–Noether theorem: the block-based watermarking must be done with a fixed  $p$ .

### B. Efficiency of a Mixture of Fundamental Solutions

This section uses the geometric property of Section III-D to calculate the efficiency per element of a detection function defined by a mixture of fundamental solutions. Suppose a family of orthonormal fundamental solutions  $\{t_j\}$  with integer indices (this is easily generalized to indices in  $\mathbb{N}^p$ ), and create the following detection function  $t(\mathbf{r}) = \sum_{j=1}^{\Omega} \omega_j t_j(\mathbf{r})$ . We have

$$\mathbb{E}_{\mathbf{R}}\{t(\mathbf{r})|\mathcal{H}_0\} = \sum_{j=1}^{\Omega} \omega_j \mathbb{E}_{\mathbf{R}}\{t_j(\mathbf{r})|\mathcal{H}_0\} = 0 \quad (63)$$

$$\text{Var}\{t(\mathbf{r})|\mathcal{H}_0\} = \sum_{j=1}^{\Omega} \omega_j^2 = 1. \quad (64)$$

The last equation gives a constraint on the weights  $\{\omega_j\}$ .

The reader must be aware of two facts. First, we have chosen here to mix some detection functions, but we could also do the mixture on the embedding functions. Second, this mixture

is *a priori* not a fundamental solution. Given this mixture, we select the best embedding function  $\mathbf{w}(\mathbf{s}) = k_w \nabla t(\mathbf{s})$ . However, it is *a priori* not true that the mixture is the best detection function knowing  $\mathbf{w}(\mathbf{s})$ . The mixture of detection functions implies a mixture of the associated embedding functions  $\mathbf{w}(\mathbf{s}) = \sum_{j=1}^{\Omega} \varpi_j \mathbf{w}_j(\mathbf{s})$ , but with different weights

$$\varpi_j = k_w \omega_j \sqrt{\eta_j(1,0)} \quad \text{and} \quad k_w = \left( \sum_{j=1}^{\Omega} \omega_j^2 \eta_j(1,0) \right)^{-1/2}.$$

Equation (23) gives the efficacy when there is no attack

$$\eta(1,0) = \sum_{j=1}^{\Omega} \omega_j^2 \eta_j(1,0). \quad (65)$$

Equation (56) gives the following efficiency per element under attack:

$$\begin{aligned} \eta(\gamma, \sigma_z) &= \left( \sum_{j=1}^{\Omega} \omega_j \varpi_j \sqrt{\eta_j(\gamma, \sigma_z)} \right)^2 \\ &= \frac{\left( \sum_{j=1}^{\Omega} \omega_j^2 \sqrt{\eta_j(1,0) \eta_j(\gamma, \sigma_z)} \right)^2}{\sum_{j=1}^{\Omega} \omega_j^2 \eta_j(1,0)} \end{aligned} \quad (66)$$

if we suppose that

$$\mathbb{E}_{\mathbf{S}}\{\mathbf{w}_j(\mathbf{s})\mathbb{E}_{\mathbf{Z}}\{\mathbf{w}_k(\gamma(\mathbf{s} + \mathbf{z}))\}\} = \frac{\delta(j-k)n}{\gamma} \sqrt{\frac{\eta_j(\gamma, \sigma_z)}{\eta_j(1,0)}}$$

that is, the functions stay orthogonal even under attack. This assumption considerably simplifies the expression of the efficiency. From Section VI-B, we know this holds for the polynomial family ( $\gamma = 1/\sqrt{1+\sigma_z^2}$ ), and for the sinusoidal family ( $\gamma = 1$ ), because  $\mathbb{E}_{\mathbf{Z}}\{\mathbf{w}_k(\gamma(\mathbf{s} + \mathbf{z}))\} \propto \mathbf{w}_k(\mathbf{s})$ .

It is quite difficult to compare mixtures of the fundamental solutions and to derive the optimum weighting. Let us denote the score  $g_M(\{\omega_j\}, \gamma, \sigma_z) = \sqrt{\eta(1,0)\eta(\gamma, \sigma_z)}$  for a mixture with weights  $\{\omega_j\}$  and  $g_P(\eta(1,0), \gamma, \sigma_z)$  the same score but for a pure fundamental solution whose efficiency is  $\eta(1,0) = \sum_{j=1}^{\Omega} \omega_j^2 \eta_j(1,0)$  when there is no noise.<sup>5</sup> These two scores are equal when there is no noise; otherwise, they have the following expressions:

$$g_M(\{\omega_j\}, \gamma, \sigma_z) = \sum_{j=1}^{\Omega} \omega_j^2 \eta_j(1,0) \gamma h_j(\gamma, \sigma_z) \quad (67)$$

$$g_P(\eta(1,0), \gamma, \sigma_z) = \eta(1,0) \gamma h(\gamma, \sigma_z) \quad (68)$$

where function  $h$  is defined in Section VI-B. If the embedder knows the parameters of the attack noise, then the

<sup>5</sup>Such a fundamental solution might not exist for all weight distributions. For instance, the polynomial family requires that  $\eta(1,0)\sigma_z^2 \in \mathbb{N}$

optimum weighting is given by a simplex optimization  $\omega_j = \delta(j - j^*)$  with  $j^* = \arg \max_j \eta_j(1,0) \gamma h_j(\gamma, \sigma_z)$ . Otherwise, we set the following criterion  $G_M(\{\omega_j\}) = \int_0^1 \int_0^{+\infty} g_M(\{\omega_j\}, \gamma, \sigma_z) d\sigma_z d\gamma$ . This represents the average performance of the mixture when no prior knowledge about the attack noise parameters is given.

For the sinusoidal family, (66) holds if  $\gamma = 1$ . The integration only made over  $\sigma_z$  gives

$$\begin{aligned} G_M(\{\omega_j\}) &= \sqrt{\frac{\pi}{2}} \sum_{j=1}^{\Omega} \omega_j^2 \sqrt{\eta_j(1,0)} \\ &\leq \sqrt{\frac{\pi}{2}} \sqrt{\eta(1,0)} = G_P(\eta(1,0)). \end{aligned} \quad (69)$$

The inequality is due to the concavity of the square root function and it holds for any weight distribution. In the same way, for the polynomial family, (66) holds if  $\gamma = (1 + \sigma_z^2)^{-1/2}$ . The integration only made over  $\gamma$  gives

$$\begin{aligned} G_M(\{\omega_j\}) &= \sum_{j=1}^{\Omega} \omega_j^2 \frac{\eta_j(1,0)}{\eta_j(1,0) + 1} \\ &\leq \frac{\eta(1,0)}{\eta(1,0) + 1} = G_P(\eta(1,0)). \end{aligned} \quad (70)$$

The inequality is due to the concavity of the function  $x \rightarrow x/(1+x)$  on  $[0, +\infty)$  and it holds for any weight distribution.

This tends to show that a pure fundamental solution is, on average, more robust than any mixture of fundamental solutions. However, this is not a general proof. We have shown this is only for the sinusoidal and the polynomial families when considering attacks such that (66) holds and when  $h(\gamma, \sigma_z)$  has a known expression.

### C. Application to DC-DM Watermarking

Mixture is a tool which renders the study of some watermarking schemes to be easier. When applied on elements of the sinusoidal family, this allows the recreation of whatever the periodic detection function is. For instance, the following weights  $\omega_j = -(-1)^j 3\sqrt{10}/\pi^2/j^2$  give the Fourier series decomposition of the SCS scheme:

$$\begin{aligned} t(s) &= -\frac{6\sqrt{5}}{\pi^2} \sum_{j=1}^{\infty} \frac{(-1)^j}{j^2} \cos(j\sqrt{\eta}s) \\ &= \frac{\sqrt{5}}{2} - (s - Q(s))^2 \frac{6\sqrt{5}}{\Delta^2} \end{aligned} \quad (71)$$

$$\begin{aligned} w(s) &= k_w \frac{6\sqrt{5}\eta}{\pi^2} \sum_{j=1}^{\infty} \frac{(-1)^j}{j} \sin(j\sqrt{\eta}s) \\ &= -(s - Q(s)) \frac{\sqrt{12}}{\Delta} \end{aligned} \quad (72)$$

with  $Q$  being a quantizer whose step is  $\Delta = 2\pi/\sqrt{\eta}$ . The application of (66) gives the efficiency of SCS under an

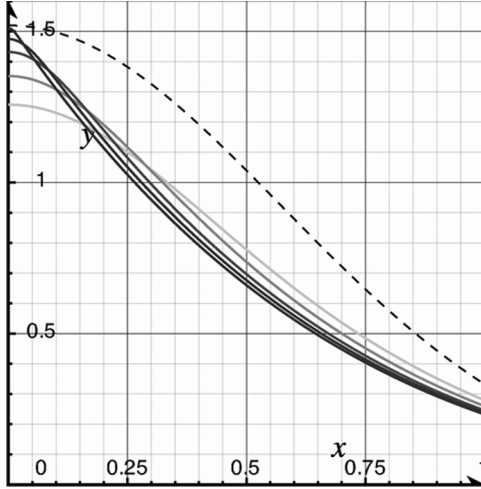


Fig. 2. Efficiency per element of the SCS scheme under the AWGN attack against  $\sigma_z$ . The gray plots are the approximations by (73) for  $j_{\max} = \{3, 5, 10, 20, 100\}$ . The dotted line is the efficiency of the sinusoidal solution with  $\eta(1, 0) = 1, 52$ .

AWGN attack, which is otherwise cumbersome to calculate with the direct expressions of  $t$  and  $w$ . Here, we simply have

$$\begin{aligned} \eta_{\text{SCS}}(1, \sigma_z) &= \frac{90\eta}{\pi^4} \cdot \frac{\left( \sum_{j=1}^{\infty} j^{-2} e^{-j^2 \eta \sigma_z^2 / 2} \right)^2}{\sum_{j=1}^{\infty} j^{-2}} \\ &= \frac{60}{\Delta^2} \left( 1 + \frac{6\sigma_z^2}{\Delta^2} - \frac{3}{\pi} \int_0^{2\pi\sigma_z^2/\Delta^2} \vartheta_3(0, e^{-\pi u}) du \right)^2 \end{aligned} \quad (73)$$

where  $\vartheta_3$  is the third Jacobi theta function. When there is no attack,  $\eta_{\text{SCS}}(1, 0) = 60/\Delta^2 = 15\eta/\pi^2 \approx 1.52\eta$ . Fig. 2 shows the efficiency per element of SCS with  $\sigma_z$  ranging from 0 to 1 for  $\eta = 1$ . It shows that the efficiency per element of a pure sinusoidal function starting from the same value (i.e.,  $\eta_{\text{SCS}}(1, 0)$ ) is largely more robust in this range of noise. However, when the variance of the noise increases, the asymptotic behavior of (73) is dominated by the first term  $j = 1$  (i.e.,  $e^{-\eta\sigma_z^2}$ ) whereas the efficiency of the previous pure sinusoidal function has stronger exponential decay  $e^{-1.52\eta\sigma_z^2}$ . In this asymptotic case, a pure sinusoidal function with efficacy  $\eta$  performs better.

In the same way, the detection function based on lattice quantizer of Section VII-A can be decomposed through a Fourier series over lattice  $\Lambda$ , whose generator matrix is  $G$

$$t(\mathbf{r}) = I(\Lambda, 2) + \sqrt{2} \sum_{\mathbf{k} \in \mathbb{N}^p} \omega_{\mathbf{k}} \cos(2\pi \mathbf{r}^T G^{-T} \mathbf{k}) \quad (74)$$

with  $\omega_{\mathbf{k}} = \sqrt{2} \text{vol}(\mathcal{V})^{-1} \int_{\mathcal{V}} \|\mathbf{r}\|^2 \cos(2\pi \mathbf{r}^T G^{-T} \mathbf{k}) d\mathbf{r}$ . This decomposition in Fourier series may not be easy to obtain except for low-dimension lattices. Yet, whatever the resulting weight distribution is, the mixture has for  $\eta(1, \sigma_z)$ ,  $g_M(\{\omega_{\mathbf{k}}\}, \gamma, \sigma_z)$ , and  $G_M(\{\omega_{\mathbf{k}}\})$  equivalent expressions as for the one dimensional case thanks to the common expression of the efficiency as shown in Appendix C. Therefore, the main conclusion is still

valid: under an AWGN attack, a pure sinusoidal solution sharing the same efficiency without noise, performs better on average.

## VIII. CONCLUSION

Rewriting classical elements of detection theory with the assumption that the watermark signal depends on the host gives us the expression of the best embedding function knowing the detector. Coupling this result with the expression of the LMP test gives a partial differential equation we call the ‘‘fundamental equation’’ of zero-bit watermarking. Its main advantage is to offer a constructive theoretical framework unifying most of the watermarking schemes that the community knows. Moreover, a side product is that the decomposition onto a family of orthogonal fundamental solutions provides an easier way to characterize the performance of DC-DM schemes.

## APPENDIX A

### LMP TEST

For a given embedding function  $\mathbf{w}$ , we derive the LMP test, whose detection function is defined as

$$t(\mathbf{r}) = \frac{k_t}{ps(\mathbf{r})} \left. \frac{\partial p(\mathbf{r}|\mathcal{H}_1)}{\partial \theta} \right|_{\theta=0} \quad (75)$$

where  $\theta \rightarrow 0$  makes function  $\mathbf{f}$  invertible  $\mathbf{s} = \mathbf{f}^{-1}(\mathbf{y})$ , and  $p(\mathbf{r}|\mathcal{H}_1) = ps(\mathbf{f}^{-1}(\mathbf{r})) |J_{\mathbf{f}^{-1}}(\mathbf{r}, \theta)|$ , with the last term being the Jacobian of  $\mathbf{f}^{-1}$ . Finally, the detection function is

$$\begin{aligned} t(\mathbf{r}) &= \frac{k_t}{ps(\mathbf{r})} \left( \nabla ps(\mathbf{f}^{-1}(\mathbf{r}))^T \frac{\partial \mathbf{f}^{-1}}{\partial \theta}(\mathbf{r}) |J_{\mathbf{f}^{-1}}(\mathbf{r}, \theta)| \right. \\ &\quad \left. + ps(\mathbf{f}^{-1}(\mathbf{r})) \frac{\partial |J_{\mathbf{f}^{-1}}(\mathbf{r}, \theta)|}{\partial \theta} \right)_{\theta=0} \\ &= \frac{k_t}{ps(\mathbf{r})} (A(\mathbf{r}) + B(\mathbf{r})). \end{aligned} \quad (76)$$

Some simple equations are

$$\mathbf{f}(\mathbf{s})|_{\theta=0} = \mathbf{s} \quad (77)$$

$$\mathbf{f}^{-1}(\mathbf{y})|_{\theta=0} = \mathbf{y} \quad (78)$$

$$\mathbf{f}^{-1}(\mathbf{y}) = \mathbf{y} - \theta \mathbf{w}(\mathbf{f}^{-1}(\mathbf{y})). \quad (79)$$

*Expression of A(r):* Deriving this last expression gives

$$\frac{\partial \mathbf{f}^{-1}}{\partial \theta}(\mathbf{y}) = -\mathbf{w}(\mathbf{f}^{-1}(\mathbf{y})) - \theta J_{\mathbf{w}}(\mathbf{f}^{-1}(\mathbf{y})) \frac{\partial \mathbf{f}^{-1}}{\partial \theta}(\mathbf{y}). \quad (80)$$

Hence

$$\left. \frac{\partial \mathbf{f}^{-1}}{\partial \theta}(\mathbf{y}) \right|_{\theta=0} = -\mathbf{w}(\mathbf{y}). \quad (81)$$

The elements of the Jacobian matrix are given by

$$\begin{aligned} [J_{\mathbf{f}^{-1}}(\mathbf{y}, \theta)](i, j) &= \frac{\partial f_i^{-1}}{\partial y_j} \\ &= \delta(i - j) - \theta \nabla w_i(\mathbf{f}^{-1}(\mathbf{y}))^T J_{\mathbf{f}^{-1}}(\mathbf{y}) \mathbf{e}_j. \end{aligned} \quad (82)$$

The simplification taking  $\theta = 0$  yields  $|J_{\mathbf{f}^{-1}}(\mathbf{y}, 0)| = 1$ , and the expression of  $A$  is as follows:

$$A(\mathbf{r}) = -\nabla ps(\mathbf{r})^T \mathbf{w}(\mathbf{r}). \quad (83)$$

*Expression of  $B(\mathbf{r})$ :* This term implies the derivative of the determinant of matrix  $J_{\mathbf{f}^{-1}}(\mathbf{r}, \theta)$  which is invertible as  $\theta \rightarrow 0$

$$\frac{\partial |J_{\mathbf{f}^{-1}}|}{\partial \theta}(\mathbf{r}, \theta) = |J_{\mathbf{f}^{-1}}(\mathbf{r}, \theta)| \text{tr} \left( J_{\mathbf{f}^{-1}}(\mathbf{r}, \theta)^{-1} \frac{\partial J_{\mathbf{f}^{-1}}}{\partial \theta}(\mathbf{r}, \theta) \right). \quad (84)$$

Taking  $\theta = 0$ , gives

$$\frac{\partial |J_{\mathbf{f}^{-1}}|}{\partial \theta}(\mathbf{r}, 0) = \text{tr} \left( \frac{\partial J_{\mathbf{f}^{-1}}}{\partial \theta}(\mathbf{r}, 0) \right). \quad (85)$$

The derivative of (82) gives the elements of matrix  $(\partial J_{\mathbf{f}^{-1}} / \partial \theta)(\mathbf{r}, \theta)$

$$\begin{aligned} \frac{\partial^2 f_i^{-1}}{\partial \theta \partial y_j}(\mathbf{r}, \theta) &= -\nabla w_i(\mathbf{f}^{-1}(\mathbf{r}))^T J_{\mathbf{f}^{-1}}(\mathbf{r}, \theta) \mathbf{e}_j \\ &\quad - \theta \frac{\partial}{\partial \theta} (\nabla w_i(\mathbf{f}^{-1}(\mathbf{r}))^T J_{\mathbf{f}^{-1}}(\mathbf{r}, \theta) \mathbf{e}_j). \end{aligned} \quad (86)$$

So that these elements are equal to  $-\nabla \mathbf{w}_i(\mathbf{r})^T \mathbf{e}_j$  when  $\theta = 0$  and, finally,  $B(\mathbf{r}) = -p_S(\mathbf{r}) \text{div}(\mathbf{w}(\mathbf{r}))$ .

#### APPENDIX B

##### MACLAURIN SERIES OF $\text{Var}\{t(r)|\mathcal{H}_1\}$ WITHOUT ATTACK

We make the Maclaurin series of  $t(s + \theta w(s))^2$ , and take the expectation

$$\begin{aligned} E_S\{t(s + \theta w(s))^2\} &= 1 + 2\theta E_S\{w(s)t'(s)t(s)\} \\ &\quad + \theta^2 E_S\{w(s)^2(t'(s)^2 + t(s)t''(s))\} + O(\theta^3). \end{aligned} \quad (87)$$

If  $t$  is an odd function, then  $t'$  and  $w = k_w t'$  are even functions. The second term of the series is null. If  $t$  is an even function, the second term is not null as shown in Table I.

*First-Order Term for Even Polynomial Function:* An even polynomial detection function means  $t(s) = \kappa_k H_k(s)$ , with  $k$  even and  $\kappa_k = k!^{-1/2}$  (probabilists' definition). Then,  $t'(s) = \kappa_k k H_{k-1}(s)$  and  $w(s) = k_w \kappa_k k H_{k-1}(s) = \kappa_{k-1} H_{k-1}(s)$ . Therefore,  $E_S\{w(s)t'(s)t(s)\} = \kappa_k^2 \kappa_{k-1} k E_S\{H_k(s)H_{k-1}(s)^2\}$ . A known formula of the square of Hermite polynomials is the following:

$$H_{k-1}(s)^2 = \sum_{\ell=0}^{k-1} \binom{k-1}{\ell}^2 \ell! H_{2k-2-2\ell}(s). \quad (88)$$

The orthogonality of the Hermite polynomial family allows us to conclude that

$$\begin{aligned} E_S\{w(s)t'(s)t(s)\} &= \kappa_k^2 \kappa_{k-1} k \binom{k-1}{k/2-1}^2 \left(\frac{k}{2} - 1\right)! k! \\ &= \frac{\sqrt{(k-1)!k!}}{\left(\frac{k}{2} - 1\right)! \left(\frac{k}{2}\right)^2}. \end{aligned} \quad (89)$$

The application of the Stirling approximation, when  $k$  is large, gives  $E_S\{w(s)t'(s)t(s)\} \approx \sqrt{2/e}(2\pi)^{-3/4} 2^{3k/2} k^{-1/4}$ . The derivation of the second-order term is tackled in the following section.

*Second-Order Term:* In a similar way, we have

$$w(s)^2 t'^2(s) = \frac{k}{(k-1)!^2} \left( \sum_{\ell=0}^{k-1} \binom{k-1}{\ell}^2 \ell! H_{2k-2-2\ell}(s) \right)^2 \quad (90)$$

whose expectation, thanks to the orthogonality feature, is simplified to

$$E_S\{w(s)^2 t'^2(s)\} = \frac{k}{(k-1)!^2} \sum_{\ell=0}^{k-1} \binom{k-1}{\ell}^4 \ell!^2 (2k-2-2\ell)!. \quad (91)$$

The second term is slightly different

$$\begin{aligned} w(s)^2 t''(s)t(s) &= \frac{k(k-1)}{k!(k-1)!} H_{k-1}(s)^2 H_k(s) H_{k-2}(s), \\ &= \frac{k^2}{k!(k-1)!} \left( \sum_{\ell=0}^{k-1} \binom{k-1}{\ell}^2 \ell! H_{2k-2-2\ell}(s) \right) \\ &\quad \left( \sum_{\ell=0}^{k-2} \frac{k-\ell-1}{k-\ell} \binom{k-1}{\ell}^2 \ell! H_{2k-2-2\ell}(s) \right) \end{aligned}$$

whose expectation is

$$\begin{aligned} E_S\{w(s)^2 t''(s)t(s)\} &= \frac{k}{(k-1)!^2} \sum_{\ell=0}^{k-2} \left(1 - \frac{1}{k-\ell}\right) \binom{k-1}{\ell}^4 \ell!^2 (2k-2-2\ell)!. \end{aligned} \quad (92)$$

*Final Expression:* Withdrawing the square of  $E_{\mathbf{R}}\{t(\mathbf{r})|\mathcal{H}_1\} = \sqrt{k}\theta + O(\theta^2)$ , we obtain

$$\begin{aligned} \text{Var}\{t(\mathbf{r})|\mathcal{H}_1\} &= 1 + 2 \text{mod}(k+1, 2) \theta \frac{\sqrt{(k-1)!k!}}{\left(\frac{k}{2}-1\right)! \left(\frac{k}{2}\right)!^2} \\ &\quad + \theta^2 \frac{k}{(k-1)!^2} \sum_{\ell=0}^{k-2} \left(2 - \frac{1}{k-\ell}\right) \binom{k-1}{\ell}^4 \ell!^2 (2k-2-2\ell)! + O(\theta^3). \end{aligned}$$

#### APPENDIX C

##### EFFICACY OF THE EXTENDED SINUSOIDAL FAMILY UNDER AWGN ATTACK

We have  $\nabla t(\mathbf{r}) = -\sqrt{2} \sin(\mathbf{r}^T \boldsymbol{\lambda}_k) \boldsymbol{\lambda}_k$ . Therefore

$$\begin{aligned} E_{\mathbf{Z}}\{\nabla t(\mathbf{r} + \mathbf{z})\} &= -\sqrt{2} (\sin(\mathbf{r}^T \boldsymbol{\lambda}_k) E_{\mathbf{Z}}\{\cos(\mathbf{z}^T \boldsymbol{\lambda}_k)\} \\ &\quad + \cos(\mathbf{r}^T \boldsymbol{\lambda}_k) E_{\mathbf{Z}}\{\sin(\mathbf{z}^T \boldsymbol{\lambda}_k)\}) \boldsymbol{\lambda}_k. \end{aligned} \quad (93)$$

The last term is null when the pdf of  $\mathbf{Z}$  is odd (i.e.,  $p_{\mathbf{Z}}(\mathbf{z}) = p_{\mathbf{Z}}(-\mathbf{z})$ ) because  $\sin(\mathbf{z}^T \boldsymbol{\lambda}_k)$  is even. Thus, if  $\mathbf{Z} \sim \mathcal{N}(\mathbf{0}, \sigma_z^2 \mathbf{I})$ , then  $E_{\mathbf{Z}}\{\nabla t(\mathbf{r} + \mathbf{z})\} = h(1, \sigma_z) t(\mathbf{r})$ , with

$$\begin{aligned} h(1, \sigma_z) &= E_{\mathbf{Z}}\{\cos(\mathbf{z}^T \boldsymbol{\lambda}_k)\} = E_{\mathbf{Z}} \left\{ \cos \left( \sum_{i=1}^p z_i \lambda_{k,i} \right) \right\} \\ &= E_{Z_1} \{ \cos(z_1 \lambda_{k,1}) \} E_{\mathbf{Z}} \left\{ \cos \left( \sum_{i=2}^p z_i \lambda_{k,i} \right) \right\} \\ &\quad - E_{Z_1} \{ \sin(z_1 \lambda_{k,1}) \} E_{\mathbf{Z}} \left\{ \sin \left( \sum_{i=2}^p z_i \lambda_{k,i} \right) \right\} \end{aligned}$$

$$= e^{-\lambda_{k,1}^2 \sigma_z^2 / 2} \mathbb{E}_{\mathbf{Z}} \left\{ \cos \left( \sum_{i=2}^p z_i \lambda_{k,i} \right) \right\}.$$

Repeating  $p - 1$  times the last two lines, we finally obtain

$$h(1, \sigma_z) = e^{-\|\lambda_k\|^2 \sigma_z^2 / 2} = e^{-\eta(1,0) \sigma_z^2 / 2}. \quad (94)$$

Therefore,  $\eta(1, \sigma_z) = \eta(1, 0) e^{-\eta(1,0) \sigma_z^2 / 2}$ .

#### ACKNOWLEDGMENT

The author would like to thank P. Comesaña Alfaro and the reviewers for their numerous corrections and suggestions for improvement. Also, thanks to S. Le Squin and J. Josse for having compared the results with their numerical simulations, and A. Guyader for numerous discussions about the test hypothesis.

#### REFERENCES

[1] I. Cox, M. Miller, and J. Bloom, *Digital Watermarking*. San Mateo, CA: Morgan Kaufmann, 2001.

[2] N. Merhav, "An information-theoretic view of watermarking embedding-detection and geometric attacks," presented at the Wavila Challenge, Barcelona, Spain, Jun. 2005. [Online]. Available: <http://www.ee.technion.ac.il/people/merhav/papers/p98.pdf>.

[3] N. Merhav and E. Sabbag, "Optimal watermarking embedding and detection strategies under limited detection resources," in *Proc. Int. Symp. Information Theory*, Seattle, WA, Jul. 2006, pp. 173–177.

[4] M. Miller, I. Cox, and J. Bloom, "Informed embedding: Exploiting image and detector information during watermark insertion," in *Proc. Int. Conf. Image Processing*, Vancouver, BC, Canada, Sep. 2000.

[5] J. Delhumeau, T. Furon, N. Hurley, and G. Silvestre, "Improved polynomial detectors for side-informed watermarking," in *Proc. Security and Watermarking of Multimedia Contents IV*, Santa Clara, CA, Jan. 2003, SPIE Electron. Imag., pp. 311–321.

[6] T. Liu and P. Moulin, "Error exponents for one-bit watermarking," in *Proc. ICASSP*, Hong-Kong, China, Apr. 2003.

[7] J. P. Andreaux, A. Durand, T. Furon, and E. Diehl, "Copy protection system for digital home networks," *IEEE Signal Process. Mag.*, vol. 21, no. 2, pp. 100–108, Mar. 2004.

[8] "Analog hole," *Wikipedia, The Free Encyclopedia* [Online]. Available: [http://en.wikipedia.org/wiki/Analog\\_hole](http://en.wikipedia.org/wiki/Analog_hole). 2006.

[9] E. Diehl and T. Furon, "Closing the analog hole," in *Proc. IEEE Int. Conf. Consumer Electronics*, 2003, pp. 52–53.

[10] E. Lin, A. Eskicioglu, R. Lagendijk, and E. Delp, "Advances in digital video content protection," *Proc. IEEE*, vol. 93, no. 1, pp. 171–183, Jan. 2005.

[11] H. V. Poor, *An Introduction to Signal Detection and Estimation*, 2nd ed. New York: Springer, 1994.

[12] P. Huber, *Robust Statistics*. New York: Wiley, 1991.

[13] Q. Cheng and T. Huang, "Robust optimum detection of transform domain multiplicative watermarks," *IEEE Trans. Signal Process.*, vol. 51, no. 4, pp. 906–924, Apr. 2003.

[14] A. Briassouli and M. Strinzis, "Locally optimum nonlinearities for DCT watermarking detection," *IEEE Trans. Image Process.*, vol. 13, no. 12, pp. 1604–16017, Dec. 2004.

[15] M. Barni, F. Bartolini, A. de Rosa, and A. Piva, "Optimum decoding and detection of multiplicative watermarks," *IEEE Trans. Signal Process.*, vol. 51, no. 4, pp. 1118–1123, Apr. 2003.

[16] X. Huang and B. Zhang, "Robust detection of transform domain additive watermarks," in *Proc. Int. Workshop Digital Watermarking*, M. Barni, Ed. Siena, Italy: Springer, 2005, vol. 3710, Lecture Notes Computer Science, pp. 124–138.

[17] T. Furon, G. Silvestre, and N. Hurley, "JANIS: Just another N-order side-informed scheme," in *Proc. Int. Conf. Image Processing*, Rochester, NY, Sep. 2002, vol. 2, pp. 153–156.

[18] L. Pérez-Freire, P. Comesaña Alfaro, and F. Pérez-González, "Detection in quantization-based watermarking: Performances and security issues," in *Security, Steganography, and Watermarking of Multimedia Contents VII*, E. Delp and P. W. Wong, Eds. San Jose, CA: SPIE and IS&T, 2005, vol. 5681, Proc. SPIE-IS&T Electron. Imaging, pp. 721–733.

[19] J. Eggers and B. Girod, *Informed Watermarking*. Norwell, MA: Kluwer, 2002.

[20] U. Erez and R. Zamir, "Achieving  $0.5 \log 1 + \text{SNR}$  on additive white gaussian noise channel with lattice encoding and decoding," *IEEE Trans. Inf. Theory*, vol. 50, no. 10, pp. 2293–2314, Oct. 2004.

[21] P. Moulin, A. Goteti, and R. Koetter, "Optimal sparse-QIM codes for zero-rate blind watermarking," in *Proc. ICASSP*, Montreal, QC, Canada, May 2004.

[22] T. Furon, J. Josse, and S. Le Squin, "Some theoretical aspects of watermarking detection," in *Proc. Security, Steganography and Watermarking of Multimedia Content*, San Jose, CA, Jan. 2006.

[23] I. Cox, J. Kilian, T. Leighton, and T. Shamos, "Secure spread spectrum watermarking for multimedia," *IEEE Trans. Image Process.*, vol. 6, no. 12, pp. 1673–1687, Dec. 1997.

[24] P. Moon and D. E. Spencer, "Theorems on separability in Riemannian  $n$ -space," *Proc. Amer. Math. Soc.*, vol. 3, pp. 635–642, 1952.

[25] F. Balado, "New geometric analysis of spread-spectrum data hiding with repetition coding, with implications for side-informed schemes," in *Proc. Int. Workshop Digital Watermarking*, M. Barni, Ed. Siena, Italy: Springer-Verlag, 2005, vol. 3710, Lecture Notes Computer Science, pp. 336–350.

[26] P. Moulin and R. Koetter, "Data hiding codes," *Proc. IEEE*, vol. 93, no. 12, pp. 2083–2126, Dec. 2005.

[27] H. S. Malvar and D. A. F. Florêncio, "Improved spread spectrum: A new modulation technique for robust watermarking," *IEEE Trans. Signal Process.*, vol. 51, no. 4, pp. 868–905, Apr. 2003.

[28] T. Kalker, "Considerations on watermarking security," in *Proc. 4th Workshop on Multimedia Signal Processing*, J.-L. Dugelay and K. Rose, Eds., Cannes, France, Oct. 2001, pp. 201–206.

[29] T. Cover and J. Thomas, *Elements of Information Theory*. New York: Wiley, 1991, Wiley Series in Telecommunications.



**Teddy Furon** received the M.S. degree in digital communications and the Ph.D. degree in signal and image processing from the Ecole Nationale Supérieure des Télécommunications de Paris, Paris, France, in 1998 and 2002, respectively.

From 1998 to 2001, he was a Research Engineer with the Security Lab of THOMSON, Rennes, France, working on digital watermarking in the framework of copy protection. He continued working on digital watermarking as a Postdoctoral Researcher at the TELE Lab of the Université

Catholique de Louvain, Louvain, Belgium. Currently, he is a Researcher with the INRIA Institute working within the TEMICS Project of the IRISA Public Research Center, Rennes, France.

Dr. Furon is a Corecipient of the IWDW'04 Best Paper Award and received the Best Young Researcher of Brittany Award in computer science in 2005.